Time Dependent Studies of a Tandem Mirror with Thermal Barriers

E. Montalvo and G.A. Emmert

November 1985

UWFDM-668

To be published in Nuclear Fusion.

FUSION TECHNOLOGY INSTITUTE

UNIVERSITY OF WISCONSIN

MADISON WISCONSIN

Time Dependent Studies of a Tandem Mirror with Thermal Barriers

E. Montalvo and G.A. Emmert

Fusion Technology Institute
University of Wisconsin
1500 Engineering Drive
Madison, WI 53706

http://fti.neep.wisc.edu

November 1985

UWFDM-668

To be published in Nuclear Fusion.

TIME DEPENDENT STUDIES OF A TANDEM MIRROR WITH THERMAL BARRIERS

E. Montalvo

G.A. Emmert

Fusion Technology Institute
1500 Johnson Drive
University of Wisconsin-Madison
Madison, Wisconsin 53706

November 1985

(Revised April 1986)

UWFDM-668

TIME DEPENDENT STUDIES OF A TANDEM MIRROR WITH THERMAL BARRIERS

E. Montalvo* and G.A. Emmert

Fusion Technology Institute, 1500 Johnson Drive
University of Wisconsin-Madison, Madison, WI 53706-1687

ABSTRACT

The time evolution of a plasma confined in a tandem mirror with thermal barriers has been studied. A physics model which describes the kinetic interactions in velocity space between the particles of the various plasma species that exist in each spatial region of the confinement and the effects of a variety of particle and energy sources applied to the plasma is given. The analysis includes particle and energy rate equations for the various species that determine the plasma confinement. It also includes quasineutrality and ambipolarity conditions which define the ambipolar potential profile along the axis of the device and expressions for the passing particle densities in each region. This model describes in a self-consistent manner the time evolution of tandem mirror confinement with thermal barriers including the steady state phase of operation. The resulting system of equations is solved numerically. Specifically, we have studied the axicell MFTF-B configuration. A possible startup scenario has been obtained. The results show the time sequence that must be followed to build a plasma from given initial conditions up to steady state situation by means of appropriately programmed particle and energy sources applied to the plasma.

*Permanent address: Institute for Fusion Studies, University of Texas, Austin, TX 78712.

1. INTRODUCTION

This work deals with the simulation of the time sequence needed to achieve a stationary situation in a tandem mirror with thermal barriers. The confinement of plasma in a tandem mirror with thermal barriers [1] is based on the magnetic configuration of the device and also on how the existing plasma species interact between themselves to originate the ambipolar potential profile that provides electrostatic confinement. During the startup of a tandem mirror with thermal barriers the particle and energy confinement of the various plasma species will evolve depending on the instantaneous values of the plasma variables. Then, to reach a given steady state operating point a careful programming of the startup scenario is necessary.

The time variation of the number of particles and the energy content for the various species of the plasma are determined, accounting for the kinetic interactions between the particles and for the external sources. The ambipolar potentials that confine the particles are determined by the quasineutrality and ambipolarity conditions at the different spatial regions of the device. These regions are maintained in contact through populations of passing particles whose densities are evaluated by employing the condition of constant distribution function along field lines. Maxwellian distribution functions are assumed for the trapped species. These equations provide with consistent model that describes the behavior of a plasma confined in a tandem mirror.

A detailed account of all the kinetic effects in a barrier tandem mirror would require solving a Fokker-Planck problem which should include all the plasma species in the device, as well as the external sources applied to the plasma. Because of the complicated structure of the electric and magnetic

fields in the device there are a variety of particle species occupying different regions of the phase space. This makes the problem non-solvable in general using the Fokker-Planck codes available to date. The approach considered here is to make detailed particle and energy balances with velocity space interactions between species taken into account by analytical models found in the literature. These models are derived either from numerical studies or from analytical solutions of simplified Fokker-Planck problems.

The time evolution of the plasma variables is simulated by integrating in time the balance equations and by solving instantaneously quasineutrality and ambipolarity equations. The problem reduces to the solution of a system of coupled ordinary differential equations which is integrated numerically subject to constraints that take the form of a system of coupled nonlinear equations to be satisfied by the ambipolar potentials at each time-step. In our treatment of the problem, no spatial effects are taken into account other than the square well profiles of magnetic fields and ambipolar potentials along the axis of the device.

We have set up a time dependent physics model to describe the evolution of a plasma confined in a tandem mirror with thermal barriers. We then make numerical simulations of the time evolution of the more relevant plasma parameters when external power and particle sources are applied to the plasma. Specifically, we consider the axicell MFTF-B reference case [2,3] configuration referred to as the axicell MARS mode of MFTF-B. In this configuration the central cell is terminated at either end by an axisymmetric mirror cell named "axicell." This axicell throttles the flow of ions from the central cell to the end cells. The central cell ions are mostly confined by the high mirror ratio provided by the axicells. There is also some electrostatic plug-

ging provided by the axicells, due to the potential peak formed by hot ions mirror-trapped at their midplanes. This hot ion population is sustained by neutral beams injected in the axicell midplane.

The higher plugging potential peak and the associated thermal barrier are inside the yin-yang cells situated at both ends of the device. These minimum-B cells act as magnetohydrodynamic (MHD) anchors to the whole system. The thermal barrier plugs include sloshing ions and the ion confining potential is produced by electron cyclotron resonance heating (ECRH) applied to the outermost sloshing ion density peak. The thermal barrier potential dip is maintained by neutral beam pumping of the ion population trapped in the potential depression. The barrier potential is further enhanced by creating a hot barrier electron population by means of additional ECRH heating applied at the yin-yang midplane. Electrical contact between the axicell/central cell combination and the minimum-B anchor cell is maintained through the transition region by a plasma of relatively low density and pressure. Additional neutral beam pumping is required to maintain a low transition region density. Axial profiles of magnetic field and ambipolar potentials are shown in Fig. 1.

This paper is organized as follows: Section 2 describes the physics model for the axicell barrier tandem mirror. Section 3 presents a possible startup scenario. Some conclusions are summarized in Section 4. Expressions for the densities of passing particles at the various axial locations are given in the Appendix.

2. TIME DEPENDENT PHYSICS MODEL

The axicell MFTF-B configuration consists basically of five different spatial regions: central cell, axicell, transition, barrier, and plug. The

velocity space is also divided into regions, with each of them containing a characteristic class of ions and electrons. Figures 2 and 3 show, respectively, the ion and electron velocity space diagrams for the MFTF-B reference case. The coordinate axes represent energy E and magnetic moment μ.

The following species are considered: central cell ions, electrons and alpha particles; axicell hot ions; transition region cold trapped ions; barrier cold trapped ions and hot electrons; and plug warm electrons and sloshing ions. The central cell ion population passes through the axicell, transition and barrier regions. Central cell electrons occupy portions of velocity space all along the device. Barrier hot electrons can reach the plug and the plug sloshing ions are bouncing between the yin-yang mirror points. In Fig. 4 sketches of the electron and ion axial density profiles are shown. The external sources acting upon them are: central cell gas, neutral beams and pellet injection, and auxiliary ion and electron heating; axicell neutral beams; transition pumping neutral beams; barrier pumping neutral beams and ECRF electron heating; and plug sloshing ion beams and ECRF electron heating. Some of these sources, although not included in the axicell MFTF-B reference case [2,3], have been included here to add flexibility in the time dependent calculations. The plasma parameters which appear in the equations are defined on the axis of the device. Radial variations are then taken into account by introducing a correction factor in the definitions of the magnetic field and the effective volume occupied by each species. We will consider radial density profiles of the form $n(r) = n_o[1 - (r/r_p)^\gamma]$, where n_o is the on-axis density, r_p is the plasma radius, and γ is an input parameter. The volume correction factor is then $c_r = \gamma^2/((\gamma + 1)(\gamma + 2))$.

Magnetic fields are calculated using the long-thin approximation:

$$B_{plasma} = B_{vacuum} (1 - \langle\beta\rangle)^{1/2} , \tag{1}$$

where $\langle\beta\rangle$ is the radially averaged value of the perpendicular beta (perpendicular plasma pressure/magnetic field pressure). The averaged value of β is defined as $\langle\beta\rangle = \beta_o c_r$, where β_o is the on-axis beta and it is assumed that the temperature has the same radial profile as the density. The plasma radius, $r_p(z)$, at a given magnetic field $B(z)$ is calculated using the equation for magnetic flux conservation,

$$r_p(z) = r_c \left(\frac{B_c}{B(z)}\right)^{1/2} , \tag{2}$$

where the central cell radius r_c is an input parameter. $B(z)$ is known at several axial locations (see Fig. 1). Some comments on the notation may be useful. The various spatial regions are denoted by the subscripts: "c" central cell, "x" axicell, "t" transition, "b" barrier, "a" plug, and "y" yin-yang (anchor). Additional subscripts give information about whether the species are ions, "i", or electrons, "e"; cold, "c", warm, "w", or hot, "h"; and trapped, "t", or passing, "p". Quantities used include densities (n), temperatures (T), volumes (V) and magnetic fields (B). Mirror ratios are denoted by $R_{i,j} = B_i/B_j$. Next we analyze the physics model used to describe the central cell, axicell, transition and anchor regions.

2.1 Central Cell

The central cell model considers two ion populations: a thermal ion species with density n_{ic}, temperature T_{ic}, and mass number A_{ic} and a thermal-

ized alpha particle population with density $n_{\alpha c}$ and temperature $T_{\alpha c} = T_{ic}$. There is also one cold electron species with density n_{ec} and temperature T_{ec}. A fraction of the thermal ion population spans the axicell, transition and barrier regions. Alpha particles are assumed to be confined in the central cell. The cold electron population spans the axicell, transition, barrier and plug regions either as a passing population or filling the entire velocity space in some regions. The central cell electron rate equation describes cold electrons all along the machine.

The rate equation describing the thermal ion density evolution is

$$\frac{dn_{ic}}{dt} = S^{g}_{abs} \frac{\langle\sigma V\rangle_{io,g}}{\langle\sigma V\rangle_{tot,g}} + S^{c}_{abs} \frac{\langle\sigma V\rangle_{io,c}}{\langle\sigma V\rangle_{tot,c}} + \frac{n_{ecx} n_{ihx}}{(n\tau)_{ihx}} \frac{2V_x}{V_c} - \langle J_{trap}\rangle_t \frac{2V_t}{V_c}$$

$$- J_{trap,b} \frac{2V_b}{V_c} + S^{t}_{abs} \frac{2V_t}{V_c} + S^{b}_{abs} \frac{2V_b}{V_c} - S^{x}_{abs} \frac{\langle\sigma V\rangle^{ic}_{cx,x}}{\langle\sigma V\rangle_{tot,x}} \frac{n_{icx}}{n_x} \frac{2V_x}{V_c} \qquad (3)$$

$$- \frac{1}{2} n^2_{ic} \langle\sigma V\rangle_{dt} - \frac{n^2_{ic}}{(n\tau)_{ic}} .$$

Central cell ions can be supplied by gas and neutral beams. The first term on the right side of Eq. (3) represents fueling by ionization of gas. S^{g}_{abs} is the gas absorption rate per unit volume, $\langle\sigma V\rangle_{io,g}$ is the gas ionization cross section due to collisions with ions and electrons, and $\langle\sigma V\rangle_{tot,g}$ is the gas total cross section assuming that the only reactions are ionization and charge exchange. All cross sections employed in this work retain their dependence on plasma temperature during build-up. Similarly, the second term represents fueling due to neutral beam injection. S^{c}_{abs} is the neutral beam absorption rate per unit volume and $\langle\sigma V\rangle_{io,c}$ and $\langle\sigma V\rangle_{tot,c}$ are the ionization and total cross sections. The third term takes into account the losses of hot ions out

of the axicell confined region. We assume (see Fig. 2) that all these ions end up in the central cell. Next, we take into account losses due to the central cell passing ions which become trapped in the transition and barrier regions. To pump out these trapped ions, the MFTF-B reference case uses charge exchange on pumping neutral beams. The sixth and seventh terms represent the source to the central cell ion population due to transition and barrier pumping beams. S^t_{abs} and S^b_{abs} are the neutral beam absorption rate in transition and barrier, per unit volume, respectively. The eighth term gives the loss of central cell particles due to the central cell passing ions that charge exchange on the axicell neutral beam. The ions resulting from this reaction are considered as axicell hot trapped ions. S^x_{abs} is the axicell neutral beam absorption rate per unit volume, n_{icx} is the axicell passing ion density, $\langle\sigma V\rangle^{ic}_{cx,x}$ and $\langle\sigma V\rangle_{tot,x}$ are the axicell neutral beam charge exchange cross section for collisions with passing ions, and total cross section, respectively, n_x is the axicell total density, and V_x and V_c are the axicell and central cell effective volumes. The ninth term gives losses due to fusion reactions. $\langle\sigma V\rangle_{dt}$ is the fusion cross section. Finally, the tenth term is the axial ion loss rate over the potential barrier ϕ_c. The central cell ion axial confinement product $(n\tau)_{ic}$ is determined according to the following considerations. Central cell ions are electrostatically confined by the potential ϕ_c and the mirror ratio $R_{xo,c}$. To calculate $(n\tau)_{ic}$, we use Pastukhov's [4] result when $\phi_c/T_{ic} \gtrsim 1$. Pastukhov's formula is valid for $\phi_c/T_{ic} >> 1$. Numerical calculations [5] show that Pastukhov's result slightly underestimates the central cell ion confinement time when $\phi_c \simeq T_{ic}$. For $\phi_c < 0$, central cell ions are only confined by the mirror ratio $R_{xo,c}$. We use the expression for the confinement product given in Ref. [6], valid for

$R_{xo,c} >> 1$. The case $\phi_c < 0$ is allowed by the model as long as $\phi_a > 0$ (see Fig. 1). For $0 \leq \phi_c/T_{ic} \leq 1$, a linear interpolation is used. For situations in which central cell ions are electrostatically confined by the axicell potential ϕ_x ($\phi_x > \phi_c$), $(n\tau)_{ic}$ is calculated using ϕ_x instead of ϕ_c. The confinement time expressions referenced above are based on the assumption that the mean free path of the particles is long compared with the device length. This assumption is not satisfied during the early stages of plasma buildup due to low central cell ion temperature. We take into account this collisional regime by adding a collisional contribution [7] to the confinement products for all values of ϕ_c/T_{ic}. Our study emphasizes the irreducible axial losses of particles in tandem mirrors including a smooth transition from the Pastukhov expression to the collisional regime result. Radial transport considerations are outside the scope of this work. In this sense our results apply to configurations in which the radial confinement time is much longer than the axial confinement time.

The central cell ion temperature rate equation is of the form

$$\frac{dT_{ic}}{dt} = \frac{2}{3n_{ic}} (S - L)_{ic} - \frac{T_{ic}}{n_{ic}} \frac{dn_{ic}}{dt} , \tag{4}$$

where $(S - L)_{ic}$ represents the central cell ion power balance. The ion power balance equation is

$$
\begin{aligned}
(S - L)_{ic} = {} & S^{g}_{abs} \frac{\langle\sigma V\rangle_{io,g}}{\langle\sigma V\rangle_{tot,g}} E_g + S^{c}_{abs} \frac{\langle\sigma V\rangle_{io,c}}{\langle\sigma V\rangle_{tot,c}} E_c + \frac{n_{ecx} n_{ihx}}{(n\tau)_{ihx}} \frac{2V_x}{V_c} (E_{\ell x} + \phi_x) \\
& - \langle J_{trap}\rangle_t \frac{2V_t}{V_c} \frac{3T_{ic}}{2} - J_{trap,b} \frac{2V_b}{V_c} \frac{3T_{ic}}{2} + S^{t}_{abs} \frac{2V_t}{V_c} [E_{nbt} - (\phi_{nbt} \\
& - \phi_x)] + S^{b}_{abs} \frac{2V_b}{V_c} [E_{nbb} - (\phi_{nbb} - \phi_x)] + \frac{1}{4} n^2_{ic} \langle\sigma V\rangle_{dt} [f_{\alpha i} E_\alpha (1 \\
& + \frac{E_r}{E_{fus}}) - E_r] - \frac{n^2_{ic}}{(n\tau)_{ic}} (\phi_c + T_{ic}) - S^{g}_{abs} \frac{\langle\sigma V\rangle_{cx,g}}{\langle\sigma V\rangle_{tot,g}} (\frac{3}{2} T_{ic} - E_g) \\
& - S^{c}_{abs} \frac{\langle\sigma V\rangle_{cx,c}}{\langle\sigma V\rangle_{tot,c}} (\frac{3}{2} T_{ic} - E_c) + P_{ic} - \frac{n_{ic} n_{ec}}{(n\tau)_{ec-ic}} \frac{3}{2} (T_{ic} - T_{ec}) \\
& - \frac{n_{icx} n_{ihx}}{(n\tau)_{icx-ihx}} (\frac{3}{2} T_{ic} - E_{ihx}) \frac{2V_x}{V_c} - S^{x}_{abs} \frac{\langle\sigma V\rangle^{ic}_{cx,x}}{\langle\sigma V\rangle_{tot,x}} \frac{n_{icx}}{n_x} \frac{3}{2} T_{ic} \frac{2V_x}{V_c} .
\end{aligned}
\tag{5}
$$

The first nine terms on the right side of Eq. (5) describe power variation due to particle gain or loss. E_g and E_c are the gas and central cell neutral beam injection energies, respectively. Axicell losses contribute with $(E_{\ell x} + \phi_x)$ where $E_{\ell x}$ is the axicell ion loss energy given by the Logan-Rensink model [8], and ϕ_x is the potential difference between axicell and central cell. Energy lost by trapping in the transition and barrier regions is obtained assuming that the average loss per trapped ion is 3/2 T_{ic}. The gain per absorbed particle from the transition pumping beam is $(E_{nbt} - (\phi_{nbt} - \phi_x))$, where E_{nbt} is the beam energy and ϕ_{nbt} is the potential drop between the axicell potential peak and the location where the beam is injected. Similarly, $(E_{nbb} - (\phi_{nbb} - \phi_x))$ is the energy gain due to the barrier pumping beam. If the beam is injected axially, as is the case of MFTF-B, ϕ_{nbb} represents the average potential drop between the axicell potential peak and the points along the anchor region where the ionization events can occur. Alpha particles born

in fusion reactions with energy E_α = 3.52 MeV slow down by collisions with the background plasma. The fraction of their energy imparted to ions is given by $f_{\alpha i}$ = 1. - 0.908 exp($-T_{ec}$/101.7) [9]. For plasma parameters relevant to reactor operation the ion heating due to collisions with alpha particles is the more important term in the ion power balance. The eighth term of Eq. (5) gives the power gain due to this effect. E_{fus} is the energy produced per fusion event (17.6 MeV) and E_r is the average reacting ion energy, $E_r \simeq 45. + 1.5\ T_{ic}$ [9]. The ninth term gives the energy lost axially by the ions [4]. The tenth and eleventh terms represent the energy loss due to charge exchange of injected gas and neutral beam, respectively; $\langle\sigma V\rangle_{cx,g}$ and $\langle\sigma V\rangle_{cx,c}$ are the charge exchange cross sections of the gas and neutral beams. The twelfth term represents the auxiliary ion cyclotron resonance heating (ICRH) applied to central cell ions.

Next, the collisional energy transfer terms are considered. The collisional energy transfer rate $\nu^{\alpha/\beta}$ from species β to species α is calculated using the expressions of Ref. [10]. Collisional terms are usually small. The first collisional term represents losses due to central cell electron drag. The second collisional term gives the gain due to collisions of the central cell ions passing through the axicell with the axicell hot ions. n_{icx} and n_{ihx} are the densities of the axicell passing and hot ions, respectively and E_{ihx} is the mean energy of the axicell hot ions. The central cell ion passing density beyond the axicell mirror peak is small, thus, the central cell model does not include collisional energy transfer with species outside the axicell region. The last term gives the energy loss due to the central cell ions passing to the axicell that charge exchange on the axicell beam. The energy loss per ion is 3/2 T_{ic}.

The cold central cell electron density is given by

$$\frac{dn_{ec}}{dt} = S^{g}_{abs} \frac{\langle\sigma V\rangle_{io,g}}{\langle\sigma V\rangle_{tot,g}} + S^{c}_{abs} \frac{\langle\sigma V\rangle_{io,c}}{\langle\sigma V\rangle_{tot,g}} + S^{x}_{abs} \frac{\langle\sigma V\rangle_{io,x}}{\langle\sigma V\rangle_{tot,x}} \frac{2V_x}{V_c}$$

$$+ S^{s}_{abs} \frac{\langle\sigma V\rangle_{io,s}}{\langle\sigma V\rangle_{tot,s}} \frac{2V_{ih}}{V_c} f_{sc} + S^{t}_{abs} \frac{\langle\sigma V\rangle_{io,t}}{\langle\sigma V\rangle_{tot,t}} \frac{1}{1 - \frac{\langle\sigma V\rangle_{cx,t}}{\langle\sigma V\rangle_{tot,t}} \frac{\langle n_{ictp}\rangle}{\langle n_t\rangle}} \frac{2V_t}{V_c}$$

$$+ S^{b}_{abs} \frac{\langle\sigma V\rangle_{io,b}}{\langle\sigma V\rangle_{tot,b}} \frac{1}{1 - \frac{\langle\sigma V\rangle^{c}_{cx,b}}{\langle\sigma V\rangle_{tot,b}} \frac{n_{icbp}}{n_b}} \frac{2V_b}{V_c} + F_{w\to c} \frac{2V_a}{V_c} - F_{c\to w} \frac{2V_a}{V_c} \tag{6}$$

$$+ F_{h\to c} \frac{2V_{eh}}{V_c} - F_{c\to h} \frac{2V_{eh}}{V_c} - \frac{n^2_{ec}}{(n\tau)_{ec}} ,$$

where V_a, V_{ih} and V_{eh} are the effective volumes occupied by the plug warm electrons, sloshing ions and barrier hot electrons, respectively. The cold electron sources result from the ionization of the central cell gas and various neutral beams. The first, second and third terms on the right side of Eq. (6) represent the ionization of the central cell gas, central cell neutral beam and axicell neutral beam, respectively. The fourth term gives the fraction of electrons produced by ionization of the anchor sloshing ion beam that end up in the cold electron species. Depending on the location of the injection point, f_{sc} varies from 1.0 to 0.0. If the injection occurs at the inside part of the anchor cell, f_{sc} = 1.0. If the injection is on the outside, f_{sc} = 0.0 and the electrons produced by ionization of the neutral beam are considered as a source for the warm electron species trapped in the plug. The fifth and sixth terms represent the sources due to cold electrons born by ionization of the pumping beams in the transition and barrier regions. The next

four terms give the fluxes of electrons across the velocity space boundaries which limit the region occupied by the cold species. $F_{w\to c}$, $F_{c\to w}$, $F_{h\to c}$ and $F_{c\to h}$ are the fluxes from warm to cold electrons, cold to warm electrons, hot to cold electrons and cold to hot electrons, respectively. These fluxes are obtained by applying the theory developed in Ref. [11] to the configuration considered here [16]. Finally, the last term is the axial loss over the electron confinement potential ϕ_e. The central cell electron axial confinement product $(n\tau)_{ec}$ is calculated similarly to $(n\tau)_{ic}$, with an electron confining potential ϕ_e.

The central cell electron temperature rate equation has the form

$$\frac{dT_{ec}}{dt} = \frac{2}{3n_{ec}} (S - L)_{ec} - \frac{T_{ec}}{n_{ec}} \frac{dn_{ec}}{dt} , \tag{7}$$

where $(S - L)_{ec}$ represents the central cell electron power balance. Electrons produced by ionization of gas and neutral beams are assumed to be born without kinetic energy. The energy from the neutral particles is carried out by the ions. The difference in potential between the ionization point and the central cell is taken into account in the power balance by adding or subtracting the appropriate energy. Collisional energy transfer between species and auxiliary ECRF heating are also considered. The central cell electron power balance is given by

$$(S - L)_{ec} = -S^{x}_{abs} \frac{\langle\sigma V\rangle_{io,x}}{\langle\sigma V\rangle_{tot,x}} \frac{2V_x}{V_c} \phi_x + S^{s}_{abs} \frac{\langle\sigma V\rangle_{io,s}}{\langle\sigma V\rangle_{tot,s}} \frac{2V_{ih}}{V_c} f_{sc}(\phi_{nbs} - \phi_x) \qquad (8)$$

$$+ S^{t}_{abs} \frac{\langle\sigma V\rangle_{io,t}}{\langle\sigma V\rangle_{tot,t}} \frac{1}{1 - \frac{\langle\sigma V\rangle_{cx,t}}{\langle\sigma V\rangle_{tot,t}} \frac{n_{ictp}}{n_t}} \frac{2V_t}{V_c} (\phi_{nbt} - \phi_x)$$

$$+ S^{b}_{abs} \frac{\langle\sigma V\rangle_{io,b}}{\langle\sigma V\rangle_{tot,b}} \frac{1}{1 - \frac{\langle\sigma V\rangle^{ic}_{cx,b}}{\langle\sigma V\rangle_{tot,b}} \frac{n_{ictb}}{n_b}} \frac{2V_b}{V_c} (\phi_{nbb} - \phi_x)$$

$$+ F_{w\to c} \frac{2V_a}{V_c} (\phi_a + T_{ew} - \phi_c) - F_{c\to w} \frac{2V_a}{V_c} (\phi_a + T_{ec} - \phi_c) + F_{h\to c} \frac{2V_{eh}}{V_c}$$

$$*(E_{\ell eh} + \frac{\phi_b - \phi_{yi}}{R_{yi,b} - 1} + \phi_b - \phi_x) - F_{c\to h} \frac{2V_{eh}}{V_c} (\frac{T_{ec}}{2} + \frac{\phi_b - \phi_{yi}}{R_{yi,b} - 1} + \phi_b$$

$$- \phi_x) - \frac{n^2_{ec}}{(n\tau)_{ec}} (\phi_e + T_{ec}) - \frac{n_{ic} n_{ec}}{(n\tau)_{ec\text{-}ic}} \frac{3}{2} (T_{ec} - T_{ic}) + P_{ec}$$

$$- \frac{n_{ecx} n_{ihx}}{(n\tau)_{ecx\text{-}ihx}} (\frac{3}{2} T_{ec} - E_{ihx}) \frac{2V_x}{V_c} - F_{c\to w} \frac{2V_a}{V_c} \frac{1}{2} (T_{ec} - T_{ew})$$

$$+ \frac{n^2_{ic}}{4} \langle\sigma V\rangle_{dt} f_{e\alpha} E_\alpha (1 + \frac{E_r}{E_{fus}}) .$$

The energy change due to electrons produced by ionization is described in the first four terms in the right side of Eq. (8). Axicell electrons must go over the potential ϕ_x to reach the central cell. Electrons produced by ionization of the sloshing ion beam can cause energy loss or gain depending on the beam injection point. ϕ_{nbs} is the potential at the injection point relative to the axicell potential peak and is defined positive when it is below the level of the axicell potential. Electrons produced by ionization of the

transition pumping beam as well as those produced by the barrier pumping beam carry energy provided that $(\phi_{nbt} - \phi_x)$ and $(\phi_{nbb} - \phi_x)$ are both positive.

The next four terms give an estimate of the change of energy due to the interactions of the central cell electrons with plug warm electrons and barrier hot electrons. It is necessary to emphasize here that the energy associated with the particle fluxes across velocity space boundaries has not yet been derived rigorously. $E_{\ell eh}$ is the mean hot electron loss energy taken to be $E_{eh}/2$ where E_{eh} is the hot electron mean energy. The average energy carried by a plug electron is $(\phi_a + T_{ew} - \phi_c)$; ϕ_a is the potential barrier, T_{ew} is the average perpendicular energy, and ϕ_c the potential difference. Similarly, the average energy carried by a cold electron going to the warm specie is $(\phi_a + T_{ec} - \phi_c)$. Cold electrons trapped in the hot barrier region have at least $(\phi_b - \phi_{yi})/(R_{yi,b} - 1)$ perpendicular energy, thus, the average energy loss per electron is taken to be $(T_{ec}/2 + (\phi_b - \phi_{yi})/(R_{yi,b} - 1) + \phi_b - \phi_x)$, where $(\phi_b - \phi_x)$ accounts for the difference in potential energy between the central cell and barrier. The energy gain per hot electron scattering into the cold region is $(E_{\ell eh} + (\phi_b - \phi_{yi})/(R_{yi,b} - 1) + \phi_b - \phi_x)$. The next term gives the axial energy loss. Each electron lost over the barrier ϕ_e carries an average energy $\phi_e + T_{ec}$. Next we have the collisional energy transfer with the central cell ions, the auxiliary RF power applied to central cell electrons and the collisional energy transfer between the axicell cold electrons and hot ions. The following term is the conduction term [12] associated with the passing central cell electrons scattering into the plug. The last term gives the electron heating due to collisions with alpha particles produced in fusion reactions where $f_{e\alpha} = 0.88 \exp(-T_{ec}/67.4)$ is the fraction of alpha particle energy going to electrons [9].

The rate equation for the density of thermalized alpha particles is

$$\frac{dn_{\alpha c}}{dt} = \frac{n_{ic}^2}{4} \langle\sigma V\rangle_{dt} f_{\alpha t} - C_{\alpha \ell} n_{\alpha c} , \tag{9}$$

where $f_{\alpha t} = 0.864 \left(1 - (B_c/B_{xo})\right)^{1/2} \exp(-T_{ec}/324.6)$ is a semi-empirical fit to the results of numerical Fokker-Planck simulations of thermalization and trapping of fusion alpha particles [13]. $C_{\alpha \ell}$ represents any mechanism which reduces the central cell alpha particle density.

The central cell model described above is solved to obtain the time evolution of densities and temperatures. Equations (3), (4), (7), and (9) are integrated to obtain n_{ic}, T_{ic}, T_{ec} and $n_{\alpha c}$, respectively. Then, by quasi-neutrality we obtain the central cell density $n_{ec} = n_c = n_{ic} + 2n_{\alpha c}$. Finally, the central cell beta parameter is given by

$$\beta_c = \frac{n_c(T_{ec} + T_{ic} + T_\alpha)}{2.5 \times 10^7 B_c^2} , \tag{10}$$

where $T_\alpha = 8.3 \times 10^{10} \langle\sigma V\rangle_{dt} E_\alpha f_{e\alpha} T_{ec}^{3/2}$ [9], represents the contribution of the suprathermal alpha particles to the central cell pressure and B_c is the central cell vacuum magnetic field.

2.2 Axicell

Two ion species are considered in the axicell: hot, trapped ions confined within the velocity space region limited by the surfaces represented by the lines $\mu B_x + \phi_x$ and $\mu\beta_{xi}$ in the E, μ diagram (see Fig. 2), and cold ions passing from the central cell. The density and mean energy of the hot species are n_{ihx}, E_{ihx} and the density and temperature of the cold species are n_{icx}, T_{ic}. The only electron species is the central cell cold electrons, with

density n_{ecx} and temperature T_{ec}. The total axicell density is n_x. The hot ion population is sustained by neutral beam injection in the axicell midplane.

The time evolution of the hot ion density is given by

$$\frac{dn_{ihx}}{dt} = S^x_{abs} \frac{\langle\sigma V\rangle_{io,x}}{\langle\sigma V\rangle_{tot,x}} - \frac{n_{ecx} n_{ihx}}{(n\tau)_{ihx}} + S^x_{abs} \frac{\langle\sigma V\rangle^{ic}_{cx,x}}{\langle\sigma V\rangle_{tot,x}} \frac{n_{icx}}{n_x} . \qquad (11)$$

The first term on the right-hand side is the ion source due to ionization of the absorbed fraction of the axicell neutral beam. $\langle\sigma V\rangle_{io,x}$ is the neutral beam ionization cross section due to collisions with electrons and the two ion populations, and $\langle\sigma V\rangle_{tot,x}$ is the total neutral beam cross section assuming that the only reactions are ionization and charge exchange with both cold and hot ions. S^x_{abs} is the axicell neutral beam absorption rate per unit volume. The second term represents the ions scattering out of the axicell. The axicell hot ion confinement product, $(n\tau)_{ihx}$, is calculated using the Logan-Rensink model [8]. This model was derived for a mirror cell with one mirror-trapped ion species and one electron species. The axicell contains two ion populations. Thus, the calculation of the axicell ion confinement time neglects losses due to cold ion drag. In the axicell MFTF-B reference case [2,3], the values of B_{xi}, B_x, B_{xo} and ϕ_x, ϕ_{xo} are such that the axicell hot ions are confined by the effective potential at the inside mirror point x_i, and therefore, the particle flux out of the axicell is an input to the central cell ion population. With the same magnetic field profile and larger ϕ_{xo} the effective potential at the outside mirror can drop below the level of the effective potential at the inside mirror. In this case the particles scattering out of the axicell will be lost from the machine. The last term gives the

particle source due to the cold ions which charge exchange on the beam. It is assumed that the resulting ion belongs to the trapped ion population.

The time evolution of the hot ion mean energy is given by

$$\frac{dE_{ihx}}{dt} = \frac{(S - L)_{ihx}}{n_{ihx}} - \frac{E_{ihx}}{n_{ihx}} \frac{dn_{ihx}}{dt} \tag{12}$$

where $(S - L)_{ihx}$ is the hot ion power balance given by

$$(S - L)_{ihx} = S^x_{abs} \frac{\langle\sigma V\rangle_{io,x}}{\langle\sigma V\rangle_{tot,x}} E_{nbx} - \frac{n_{ecx} n_{ihx}}{(n\tau)_{ihx}} E_{\ell x} - S^x_{abs} \frac{\langle\sigma V\rangle^{ih}_{cx,x}}{\langle\sigma V\rangle_{tot,x}} \frac{n_{ihx}}{n_x}$$

$$(E_{ihx} - E_{nbx}) - \frac{n_{icx} n_{ihx}}{(n\tau)_{icx-ihx}} (E_{ihx} - \frac{3}{2} T_{ic}) - \frac{n_{ecx} n_{ihx}}{(n\tau)_{ecx-ihx}} (E_{ihx} \tag{13}$$

$$- \frac{3T_{ec}}{2}) + S^x_{abs} \frac{\langle\sigma V\rangle^{ic}_{cx,x}}{\langle\sigma V\rangle_{tot,x}} \frac{n_{icx}}{n_x} E_{nbx} .$$

The first term on the right side of Eq. (13) gives the energy gain due to ionization of the axicell neutral beam. E_{nbx} is the beam injection energy. The second term is the energy loss due to scattering out of the confined region. $E_{\ell x}$ is given in Ref. [8]. The third term represents the energy loss due to hot ions that charge exchange with the neutral beam where $\langle\sigma V\rangle^{ih}_{cx,x}$ is the appropriate cross section for this reaction. The fourth and fifth terms are the energy loss rates due to collisions with central cell passing ions and electrons, respectively. Finally the sixth term represents the source of energy due to cold ions which charge exchange on the beam and become trapped with average energy E_{nbx}.

The axicell beta is defined by

$$\beta_x = \frac{n_x T_{ec} + n_{icx} T_{ic} + 0.9\, E_{ihx} n_{ihx}}{2.5 \times 10^7\, B_x^2} , \tag{14}$$

where the factor 0.9 in the hot ion pressure contribution accounts for the anisotropy of the hot ion distribution [3], and B_x is the vacuum axicell magnetic field at the midplane. The beta parameters at the inboard and outboard axicell mirror peaks are $\beta_{xi} \simeq 0$ and $\beta_{xo} \simeq 0$, respectively.

The potential at the axicell midplane is calculated from quasineutrality

$$n_{ecx} = n_{icx} + n_{ihx} , \tag{15}$$

where n_{ihx} is obtained from the numerical integration of Eq. (11); the passing ion and electron densities at the axicell midplane, n_{icx} and n_{ecx} are calculated in the Appendix.

To calculate the central cell passing ion density at points outside the axicell, we need to know the potential drop from the axicell midplane to the axicell outboard mirror, ϕ_{xo}. This point contains cold passing ions and electrons. In addition, a fraction of the transition trapped ions spans the outside axicell region. The transition trapped ion density is determined by a balance between trapping and pumping rates. A model to calculate the trapped density point by point is not available. To estimate the trapped density at the axicell outside mirror, the ratio of the total density and the passing density, g_{xo}, is taken as input data [3]. The potential ϕ_{xo} is calculated solving the quasineutrality condition,

$$g_{xo} n_{ipxo} = n_{exo} , \tag{16}$$

where n_{ipxo} and n_{exo} are the passing ion density and electron density at the axicell outboard mirror (see Appendix). For cases in which $\phi_c < \phi_x$ we take $n_{ipxo} = 0$.

2.3 Transition Region

The transition region connects the axicell with the anchor cell. This is a region of relatively low plasma density. We consider two cold ion species: central cell ions passing over the axicell magnetic field peak, with density n_{ictp}, and trapped ions with density n_{ictt} which are produced when the passing species collisionally trap in this region. Both species are assumed to be at the central cell temperature T_{ic}. The trapped species is pumped out by charge exchange with neutral beams injected in the transition region. The only electron species are central cell electrons with density n_{ect} and temperature T_{ec}. The transition region has quite variable density, potential, and magnetic field spatial profiles. Thus, to describe the plasma in this region with some accuracy an axial dependent model would be needed. Here it is assumed that the trapped ion density of the transition region can be represented by an averaged quantity $\langle n_{ictt} \rangle$. The coefficients of the rate equation that gives the time evolution of the average density $\langle n_{ictt} \rangle$ are calculated using averaged magnetic fields and potentials assuming parabolic profiles.

The time evolution of the transition region density is given by

$$\frac{d}{dt} \langle n_{ictt} \rangle = \langle J_{trap} \rangle_t - \nu_{cx,t} \langle n_{ictt} \rangle . \tag{17}$$

The first term of the right-hand side gives the trapping rate [12] of passing

ions which scatter into the potential depression per unit volume. The second term represents the loss rate due to charge exchange with neutral beams injected into the transition region. The requirement that ions produced by ionization and charge exchange of this beam be passing ions, i.e., that they be in the transition loss cone at the injection point, limits the minimum energy and the maximum injection angle of the pumping neutral beam. There are several reactions that can happen to neutrals absorbed by the plasma: (1) ionization due to a collision with a passing or trapped ion or an electron (the products are a new ion which appear in the passing region and an electron). (2) Charge exchange due to collision with passing ions. This reaction produces another passing ion and a neutral atom which is in the passing region. It is assumed here that this neutral is equivalent to a newly injected one. (3) Charge exchange with a trapped ion. This is a pumping event because a trapped ion is replaced by a passing one. The resulting neutrals tend to have fairly large perpendicular velocities. It is assumed that these neutrals leave the machine without undergoing secondary reactions. Then, the probability of pumping event per absorbed neutral is

$$P_{p,t} = \frac{\langle \sigma V \rangle_{cx,t}}{\langle \sigma V \rangle_{tot,t}} \frac{\langle n_{ictt} \rangle}{\langle n_t \rangle} \frac{1}{1 - \frac{\langle \sigma V \rangle_{cx,t}}{\langle \sigma V \rangle_{tot,t}} \frac{\langle n_{ictp} \rangle}{\langle n_t \rangle}} , \tag{18}$$

where $\langle n_{ictp} \rangle$ and $\langle n_t \rangle$ are the average passing and total transition densities, respectively, and $\langle \sigma V \rangle_{cx,t}$ and $\langle \sigma V \rangle_{tot,t}$ are the charge exchange and total transition beam cross sections. The total cross section includes charge exchange and ionization due to collisions with ions and electrons.

The central cell electron source per neutral absorbed in the transition region is given by

$$P_{e,t} = \frac{\langle\sigma V\rangle_{io,t}}{\langle\sigma V\rangle_{tot,t}} \frac{1}{1 - \frac{\langle\sigma V\rangle_{cx,t}}{\langle\sigma V\rangle_{tot,t}} \frac{\langle n_{ictp}\rangle}{\langle n_t\rangle}} , \tag{19}$$

where $\langle\sigma V\rangle_{io,t}$ is the neutral beam ionization cross section due to collisions with ions and electrons. It is assumed that all electrons born in the transition end up in the central cell population. Finally, every absorbed neutral in the transition produces one central cell ion.

The pumping frequency per trapped ion can be written as

$$\nu_{cx,t} = S^t_{abs} \cdot \frac{P_{p,t}}{\langle n_{ictt}\rangle} , \tag{20}$$

where S^t_{abs} is the transition neutral beam absorption rate per unit volume. To obtain the average potential $\langle\phi_t\rangle$, we use quasineutrality,

$$\langle n_{ect}\rangle = \langle n_{ictt}\rangle + \langle n_{ictp}\rangle , \tag{21}$$

where $\langle n_{ect}\rangle$ and $\langle n_{ictp}\rangle$ are the electron and passing ion average densities in the transition region, respectively. Expressions to calculate $\langle n_{ect}\rangle$ and $\langle n_{ictp}\rangle$ are given in the Appendix. For cases in which $\phi_c < \phi_x$ we take $\langle n_{ictp}\rangle = 0$. The trapped ion density $\langle n_{ictt}\rangle$ is calculated from the integration of Eq. (17).

The average transition region beta is given by

$$\langle\beta_t\rangle = \frac{\langle n_t\rangle(T_{ec} + R_{t,xo}T_{ic})}{2.5 \times 10^7 \langle B_t\rangle^2} , \tag{22}$$

where $R_{t,xo}T_{ic}$ is assumed to be the perpendicular ion temperature in the transition region and $\langle B_t \rangle$ is the average vacuum magnetic field. The average pumping parameter is defined as the ratio of the total density to the ion passing density, $\langle g_t \rangle = \langle n_t \rangle / \langle n_{ictp} \rangle$ with $\langle n_t \rangle = \langle n_{ictp} \rangle + \langle n_{ictt} \rangle$.

2.4 Anchor Region

The plugging potential peak and the adjacent thermal barrier are located in the minimum-B anchors at both ends of the device. There are several different species of trapped and passing particles considered in the barrier-plug region. A hot, sloshing-ion population with double peaked axial density profile spans the anchor region. This ion species has its minimum density at the yin-yang midplane and its outboard peak at the plug point (a). It is confined in the velocity space region limited by the lines $E = \mu B_a + \phi_c$ and $E = \mu B_{yo} - \phi_e$, as shown in Fig. 2. Cold passing ions from the central cell pass through the barrier in their transit through the machine. The passing ion density falls to zero at the plug point. A fraction of these passing ions is trapped by Coulomb collisions in the barrier potential depression. This produces a cold trapped ion species centered at the barrier midplane. The trapped ion density falls to zero at the point (a) where the potential maximum occurs.

Cold passing electrons from the central cell span the whole machine. Their density falls to zero at the outboard yin-yang mirror since this is where the absolute potential minimum occurs. Centered at the plug, there is a population of warm, trapped electrons sustained by ECRH heating applied at the plug. A fraction of this warm electron population passes through the barrier midplane. Additional ECRH heating applied at the yin-yang midplane heats the warm electron species and creates a new population of hot electrons centered at the barrier midplane. In our model it is assumed that the warm plug

electrons passing to the barrier reach the hot electron temperature and are included as part of the barrier hot electron population. Barrier hot electrons pass through the plug and their density falls to zero at the outboard yin-yang mirror.

The neutral beams injected into the barrier-plug include the high-energy sloshing-ion beam, incident perpendicular to the axis at the point where the plug is formed, and a high-energy pumping beam designed to pump out the warm trapped ions, which would otherwise build up in the potential well in the barrier. In the axicell MFTF-B design [2,3] the barrier pumping beam is injected axially. Our model includes the option of the sloshing ion beam being injected in the inboard side of the barrier at the point where the hot ion density peaks. The notation used for the densities and temperatures, or average energies, of the various species considered is as follows. Barrier cold passing and trapped ions have densities n_{icbp} and n_{icbt}, respectively, and are at the central cell ion temperature, T_{ic}. Sloshing ions at the plug have density n_{iha} and mean energy E_{iha} and at the barrier point their density is given by n_{ihb} with the same mean energy E_{iha}. The densities of cold passing electrons at the barrier and plug are given by n_{ecb} and n_{eca}, respectively. Hot electrons at the barrier have density n_{ehb} and mean energy E_{ehb} and at the plug their density is n_{eha} with the same mean energy E_{ehb}. Finally, the plug warm electron density and temperature are denoted by n_{ewa} and T_{ew}, respectively.

2.4.1 Thermal Barrier Model

Two species are trapped in the barrier and are described by means of rate equations: cold trapped ions and hot electrons. The cold trapped ion density evolution is given by

$$\frac{dn_{icbt}}{dt} = J_{trap,b} - \nu_{cx,b} n_{icbt} \cdot \tag{23}$$

The first term on the right-hand side gives the trapping rate [12] of passing ions which scatter into the potential barrier per unit volume. The second term gives the loss rate due to charge exchange with the pumping neutral beam. If the beam is injected in the axial direction, as is the case of MFTF-B, the requirement on the beam to pump particles out to the central cell is $\phi_a > E_{nbb} > \phi_b$, where E_{nbb} is the barrier neutral beam injection energy, ϕ_b is the barrier potential and ϕ_a is the plug potential. For other than axial injection, the neutral beam injection energy and injection angle must belong to the passing region of the velocity space at the injection point.

We assume that the neutral beam atoms absorbed by the barrier plasma either charge exchange with the barrier ions or are ionized by collisions with barrier ions and electrons. Any ionization reaction produces a passing ion and a cold electron. Charge exchange reactions with sloshing ions result in passing ions and hot neutrals. It is assumed that these hot neutrals escape without further interactions. Charge exchange reactions with cold trapped ions replace trapped ions with passing ions and produce neutrals which are assumed to leave the plasma. Finally, a fraction of the absorbed neutrals charge exchange with cold passing ions, producing neutrals which are in the passing region. We make the approximation that these neutral particles react with the barrier plasma with the same cross sections as the injected neutral particles. As a result of all these processes, the barrier pumping beam influences the particle balance of several species. The central cell electron source per absorbed barrier neutral is given by

$$P_{e,b} = \frac{\langle\sigma V\rangle_{io,b}}{\langle\sigma V\rangle_{tot,b}} \frac{1}{1 - \frac{\langle\sigma V\rangle^{c}_{cx,b}}{\langle\sigma V\rangle_{tot,b}} \frac{n_{icbp}}{n_b}} , \tag{24}$$

where $\langle\sigma V\rangle_{io,b}$ is the ionization cross section due to collision with every species of electrons and ions weighted with the appropriate density fraction, $\langle\sigma V\rangle^{c}_{cx,b}$ is the cold ion charge exchange cross section off the neutral beam and $\langle\sigma V\rangle_{tot,b}$ is the total cross section which includes ionization and charge exchange reactions. The sloshing ion loss due to charge exchange with the barrier neutral beam is given by

$$P_{h,cx} = \frac{\langle\sigma V\rangle^{h}_{cx,b}}{\langle\sigma V\rangle_{tot,b}} \frac{n_{ihb}}{n_b} \frac{1}{1 - \frac{\langle\sigma V\rangle^{c}_{cx,b}}{\langle\sigma V\rangle_{tot,b}} \frac{n_{icbp}}{n_b}} , \tag{25}$$

where $\langle\sigma V\rangle^{h}_{cx,b}$ is the hot ion charge exchange cross section off the neutral beam. Every absorbed neutral in the barrier produces one central cell ion. Finally, the charge exchange loss of barrier cold trapped ions per absorbed neutral is given by

$$P_{p,b} = \frac{\langle\sigma V\rangle^{c}_{cx,b}}{\langle\sigma V\rangle_{tot,b}} \frac{n_{icbt}}{n_b} \frac{1}{1 - \frac{\langle\sigma V\rangle^{c}_{cx,b}}{\langle\sigma V\rangle_{tot,b}} \frac{n_{icbp}}{n_b}} . \tag{26}$$

The pumping frequency per trapped ion, $\nu_{cx,b}$ (Eq. 23) can then be written as

$$\nu_{cx,b} = S^{b}_{abs} \cdot \frac{P_{p,b}}{n_{icbt}} , \tag{27}$$

where S^{b}_{abs} is the barrier neutral beam absorption rate per unit volume.

The hot, barrier electron density evolution is given by

$$\frac{dn_{ehb}}{dt} = F_{c\to h} - F_{h\to c} + F_{w\to h} \cdot \frac{V_a}{V_{eh}} - F_{h\to w} \frac{V_a}{V_{eh}} . \tag{28}$$

The terms on the right-hand side of Eq. (28) are the fluxes of electrons collisionally exchanged between the various electron species across their boundary surface's velocity space (see Fig. 3). The expressions for the fluxes are those of Ref. [11] applied to the MFTF-B configuration [16]. $F_{c\to h} - F_{h\to c}$ is the net flux between the hot barrier electrons and the cold passing electrons in the barrier. $F_{w\to h} - F_{h\to w}$ is the net flux between the warm electrons at the plug and the hot, barrier electrons passing to the plug. V_a and V_{eh} are the effective volumes occupied by the warm and hot electrons, respectively. Equation (28) assumes that $B_{yo} > B_{yi}$ (see Fig. 3) and therefore there is not a direct flux of hot electrons out of the device.

The time evolution of the hot electron mean energy is given by

$$\frac{dE_{ehb}}{dt} = \frac{(S - L)_{ehb}}{n_{ehb}} - \frac{E_{ehb}}{n_{ehb}} \frac{dn_{ehb}}{dt} , \tag{29}$$

where $(S - L)_{ehb}$ represents the hot electron power balance given by

$$(S - L)_{ehb} = F_{c\to h} \left(\frac{T_{ec}}{2} + \frac{\phi_b - \phi_{yi}}{R_{yi,b} - 1}\right) - F_{h\to c} \left(E_{\ell eh} + \frac{\phi_b - \phi_{yi}}{R_{yi,b} - 1}\right) + F_{w\to h} \left(R_{b,a} T_{ew}\right. \tag{30}$$

$$\left. + E_{av} - \phi_a\right) \frac{V_a}{V_{eh}} - F_{h\to w} \left(E_{\ell eh} + E_{av} - \phi_a\right) + P_{eb} - P_{syn,b} .$$

The energy factors associated with each flux term represent an estimate of the average energy involved in the process of particle exchange between species. The particle exchange between cold and hot electrons occurs in the barrier region. Cold electrons scattering into the hot barrier electron region have at least $(\phi_b - \phi_{yi})/(R_{yi,b} - 1)$ perpendicular energy and their average energy is taken to be $(T_{ec}/2 + (\phi_b - \phi_{yi})/(R_{yi,b} - 1))$. Similarly, the average loss of energy due to hot electrons scattering out of the trapped region is assumed to be $(E_{\ell eh} + (\phi_b - \phi_{xi})/(R_{yi,b} - 1))$, where $E_{\ell eh}$ is the mean hot electron loss energy, $E_{\ell eh} \simeq E_{ehb}/2$. The particle exchange between hot and warm electrons occurs in the plug region. The average energy gain per warm electron scattering into the hot electron population is estimated to be $(R_{b,a}T_{ew} + E_{av} - \phi_a)$. The factor $R_{b,a}$ has been introduced [12] to correct the temperature because warm plug electrons are not mirror-trapped but they are located in a magnetic hill with respect to the barrier point. ϕ_a represents the potential energy difference between the plug and barrier regions and the quantity E_{av} gives an estimate of the minimum energy needed by the warm electrons to pass over the potential barrier and is estimated by

$$E_{av} = \frac{\phi_a}{1 - R_{b,a}} f_{rf} + \left(\frac{\phi_b - \phi_{yi}}{R_{yi,b} - 1} + \phi_a\right)(1 - f_{rf}) , \qquad (31)$$

where f_{rf} is a parameter that takes values between zero and one ($f_{rf} \to 1$ implies that the energy is mostly perpendicular) and we have assumed $f_{rf} = 0.5$. Unfortunately, the value of this parameter is crucial in the evaluation of the RF power applied to the barrier and plug plasmas. The energy loss per hot electron scattering out of the trapped region is taken to be $(E_{\ell eh} + E_{av} -$

ϕ_a). The last two terms of Eq. (30) are the ECRH power, P_{eb}, and the synchrotron radiation losses given in Ref. [14].

In addition to the cold trapped ions and hot electrons described above, the barrier contains several passing populations. The sloshing ion density at the barrier, n_{ihb}, depends not only on the magnetic field and potential axial profiles but actually is closely related to the characteristics and location of both the sloshing ion neutral beam and barrier pumping neutral beam. We have chosen to give n_{ihb} as a fraction (f_s) of the plug density. This fraction should be evaluated by appropriate numerical studies. Expressions to calculate the density of central cell ions passing over the barrier, n_{icbp} and cold electron density, n_{ecb}, are given in the Appendix. For cases in which $\phi_c < \phi_x$, we take $n_{icbp} = 0$.

The beta parameter at the barrier is given by

$$\beta_b = \frac{0.8\, n_{ehb}E_{ehb} + n_{ecb}T_{ec} + 0.9\, n_{ihb}E_{iha}R_{b,a} + n_{icb}T_{ic}R_{b,yi}}{2.5 \times 10^7\, B_b^2} . \qquad (32)$$

The factor 0.8 in the hot electron pressure accounts for the anisotropy of the hot electron distribution function [3]. Similarly, the factor 0.9 in the sloshing ion pressure accounts for the anisotropy of the sloshing ion distribution. The mirror ratio factor in the hot and cold ion pressure terms takes into account the effect of μ conservation along field lines on the respective perpendicular energies. B_b is the vacuum barrier magnetic field and n_{icb} is the total cold ion density. The pumping parameter

$$g_b = 1 + \frac{n_{icbt}}{n_{icbp}} , \tag{33}$$

gives a measure of the trapped cold ions.

The barrier ambipolar potential is obtained from barrier quasineutrality,

$$n_{ecb} + n_{ehb} = n_{icbt} + n_{icbp} + n_{ihb} \tag{34}$$

where n_{icbt} and n_{ehb} are obtained by numerical integration of Eqs. (23) and (28), respectively. In order to solve Eq. (34) we need to know the value of the potential at the anchor inboard peak, ϕ_{yi}. Neither hot electrons nor sloshing ions reach the inner anchor peak. There are cold electrons, cold ions passing from the central cell and cold ions trapped in a velocity space zone which overlaps the transition and barrier regions. The potential ϕ_{yi} would be obtained by solving the quasineutrality condition at the point y_i. The expressions for the density of the passing species are similar to those of the barrier (see Appendix). The ion trapped density, however, cannot be determined with a model that lacks axial dependence because this density depends on how the pumping mechanisms applied at the transition and barrier act on the barely trapped ions spanning both regions. We will assume that the potential ϕ_{yi} is a given fraction of the barrier potential [3].

2.4.2 Plug Model

The region where the plugging potential is formed contains sloshing ions and three electron populations: warm electrons confined to the plug region and electrons passing from the central cell (cold) and barrier (hot) regions. The evolution of the sloshing ion density is given by

$$\frac{dn_{iha}}{dt} = S^s_{abs} \frac{\langle\sigma V\rangle_{io,s}}{\langle\sigma V\rangle_{tot,s}} - \frac{n^2_{iha}}{(n\tau)_{iha}}$$

$$- S^b_{abs} \frac{\langle\sigma V\rangle^h_{cx,b}}{\langle\sigma V\rangle_{tot,b}} \frac{n_{ihb}}{n_b} \frac{1}{1 - \frac{\langle\sigma V\rangle^c_{cx,b}}{\langle\sigma V\rangle_{tot,b}} \frac{n_{icbp}}{n_b}} \frac{V_b}{V_{ih}} . \tag{35}$$

The first term on the right side gives the ion source due to ionization of the sloshing ion neutral beam. S^s_{abs} is the absorption rate per unit volume of the neutral beam that sustains the sloshing ions. The ionization cross section $\langle\sigma V\rangle_{io,s}$ takes into account collisions with ions and electrons and the total cross section $\langle\sigma V\rangle_{tot,s}$ includes ionization and charge exchange reactions.

The second term represents the loss of sloshing ions due to ions scattering out of the confined region in velocity space, bounded by the surfaces represented by the lines $E = \mu B_a + \phi_c$ and $E = \mu B_{yo} - \phi_e$ (see Fig. 2). Ions scattering out of the hot region are lost from the device. For parameters near steady state, the injection energy of the sloshing beam E_{nbs} is in the trapped velocity space region and the confinement time multiplied by the density is given by [2]

$$(n\tau)_{iha} = 2.23 \times 10^{10} E^{3/2}_{nbs} \log_{10} R_{eff,s} , \tag{36}$$

where $R_{eff,s} = R_{yo,a}/[1 + (\phi_e + \phi_c)/E_{nbs}]$. This expression for $(n\tau)_{iha}$ requires that the beam is injected in the trapped region. In some situations far from steady state, magnetic fields and potentials are such that the beam is in the loss region. It is assumed here that the sloshing ion confinement time can then be represented by the transit time of sloshing ions in the anchor region,

$$\tau_t = 2.28 \times 10^{-8} \left(\frac{A_{nbs}}{E_{nbs}}\right)^{1/2} L_{eff,s} \,, \tag{37}$$

where A_{nbs} and E_{nbs} are the neutral mass number and injection energy, respectively, and $L_{eff,s}$ is the hot ion species effective length. If, during the calculation of the potentials ϕ_c and ϕ_e, we obtain values such that $\phi_e + \phi_c < 0$, it is assumed that Eq. (36) is still applicable with $R_{eff,s} = R_{yo,a}$. The calculation of $(n\tau)_{iha}$ described above covers all the situations which can appear when time evolution of the plasma parameters is considered and gives a rough estimate of the ion confinement time that permits evaluation of the neutral beam power required at the anchor region.

The third term on the right hand side of (35) represents the charge exchange losses with the barrier pumping neutral beam. It is assumed that this process only occurs at the barrier where the density of sloshing ions is n_{ihb}. V_b and V_{ih} are the effective volumes associated with the barrier region and the sloshing ion region, respectively.

The time evolution of the sloshing ion mean energy is given by

$$\frac{dE_{iha}}{dt} = \frac{(S - L)_{iha}}{n_{iha}} - \frac{E_{iha}}{n_{iha}} \frac{dn_{iha}}{dt} \,, \tag{38}$$

where $(S - L)_{iha}$ represents the sloshing ion power balance given by

$$(S - L)_{iha} = S^s_{abs} \frac{\langle\sigma V\rangle_{io,s}}{\langle\sigma V\rangle_{tot,s}} E_{nbs} - S^s_{abs} \frac{\langle\sigma V\rangle_{cx,s}}{\langle\sigma V\rangle_{tot,s}} (E_{iha} - E_{nbs}) - \frac{n^2_{iha}}{(n\tau)_{iha}} E_{\ell ih}$$

$$- S^b_{abs} \frac{\langle\sigma V\rangle^h_{cx,b}}{\langle\sigma V\rangle_{tot,b}} \frac{n_{ihb}}{n_b} \frac{1}{1 - \frac{\langle\sigma V\rangle^c_{cx,b}}{\langle\sigma V\rangle_{tot,b}} \frac{n_{icbp}}{n_b}} \frac{V_b}{V_{ih}} E_{iha} \qquad (39)$$

$$- \frac{n_{ewa} n_{iha}}{(n\tau)_{ew \to ih}} (E_{iha} - \frac{3}{2} T_{ew}) \frac{V_a}{V_{ih}} .$$

The first term on the right hand side gives the power input due to ionization of the sloshing neutral beam. The second represents the power loss or gain associated with the ions which charge exchange with the sloshing ion neutral beam. The third term gives the scattering losses. $E_{\ell ih}$ is the average energy of ions scattering out of the confined region and is approximated by

$$E_{\ell ih} = \frac{1}{2} \left(\frac{\phi_e + \phi_c}{R_{yo,a} - 1} + E_{iha}\right) .$$

The fourth term gives the power loss due to ions that charge exchange with the barrier pumping beam. The fifth term is the collisional energy transfer rate with the warm electron species. If the beam is injected at the point where the sloshing ion species peaks at the inboard side of the anchor region, the injection energy is corrected by the potential difference between the injection point and the plug, $(\phi_c + \phi_x - \phi_{nbs})$ where ϕ_{nbs} is the potential at the injection point relative to the axicell potential peak. To calculate ϕ_{nbs}, quasineutrality at the injection point needs to be solved. At this point there are two electron species, cold passing electrons from the central cell and hot, barrier electrons. Their densities are calculated from the condition

of constant distribution function along field lines. There are also three ion species, sloshing ions, cold passing ions and trapped ions. The sloshing ion axicell density profile is approximately symmetric about the barrier midplane. An expression to calculate the cold passing ion density is given in the Appendix. The cold trapped ion density cannot be evaluated with a model without axial dependence. We have chosen to fix the value of ϕ_{nbs} as a fraction of the barrier potential ϕ_b.

Next we describe the warm electron population. The warm electron density rate equation is given by

$$\frac{dn_{ewa}}{dt} = S^s_{abs} \frac{\langle\sigma V\rangle_{io,s}}{\langle\sigma V\rangle_{tot,s}} f_{sw} \frac{V_{ih}}{V_a} + F_{h\to w} - F_{w\to h} + F_{c\to w} - F_{w\to c} \,. \qquad (40)$$

The first term in the right side of (40) gives the fraction of electrons produced by ionization of the anchor sloshing ion beam that ends up in the warm population. Depending on the location of the injection point f_{sw} takes values from 0.0 to 1.0. If the injection point is at the inboard side of the anchor, f_{sw} = 0.0. We assume that $f_{sc} + f_{sw} = 1.0$, where f_{sc} is the fraction of electrons that ends up in the cold population. The remaining terms are the flux of electrons collisionally exchanged between the various electron species that exist in the plug region. The expressions for the fluxes are those of Ref. [11] adapted to the configuration of the axicell MFTF-B [16].

The warm electron temperature rate equation is

$$\frac{dT_{ew}}{dt} = \frac{2}{3n_{ewa}} (S - L)_{ew} - \frac{T_{ew}}{n_{ewa}} \frac{dn_{ewa}}{dt} \,, \qquad (41)$$

where $(S - L)_{ew}$ represents the warm electron power balance given by

$$(S - L)_{ew} = S^{s}_{abs} \frac{\langle\sigma V\rangle_{io,s}}{\langle\sigma V\rangle_{tot,s}} f_{sw} \frac{V_{ih}}{V_a} (\phi_c - \phi_x + \phi_{nbs}) + F_{h\to w} (E_{\ell eh} + E_{av})$$

$$- F_{w\to h} (R_{b,a} T_{ew} + E_{av}) + F_{c\to w} (T_{ec} + \phi_a) - F_{w\to c} (T_{ew} + \phi_a) \qquad (42)$$

$$- F_{c\to w} \frac{1}{2} (T_{ew} - T_{ec}) + P_{ea} - P_{syn,a} - \frac{n_{ewa} n_{iha}}{(n\tau)_{ew\to ih}} (\frac{3}{2} T_{ew} - E_{iha}) .$$

The first term in the right side gives the contribution of electrons produced by ionization of the sloshing ion neutral beam. The factor $(\phi_c - \phi_x + \phi_{nbs})$ represents the potential difference between the point of injection and the plug peak. ϕ_{nbs} is positive when it is below the axicell potential and negative otherwise. The next four terms given an estimate of the energy transfer due to collisional particle exchanges. As noted also in the central cell and barrier sections, this analysis is not rigorous, but it is expected that it will provide a reasonable estimate of the power balance terms related with fluxes of particles. The hot and warm electron exchange occurs at the plug region. Hot electrons scattering into the plug carry an average energy $(E_{\ell eh} + E_{av})$, where $E_{\ell eh} \simeq E_{ehb}/2$ and E_{av} is given in Eq. (31). The average energy of warm electrons escaping to the hot region is $R_{b,a} T_{ew} + E_{av}$, where $R_{b,a}$ corrects for the fact that warm electrons are confined in a magnetic hill [12] and E_{av} is the representative energy of their boundary contour. The cold and warm electron particle exchange occurs in the plug region. Warm electrons scattering into the cold region have at least an energy ϕ_a and an average kinetic energy T_{ew}. Similarly, the gain of energy per cold electron trapped in the plug is $T_{ec} + \phi_a$. The sixth term of Eq. (42) is the convection loss [12] associated with the cold electron species. P_{ea} is the RF power applied to the plug. The synchrotron radiation loss is given in Ref. [14]. The last

term is the collisional energy transfer rate with the sloshing ion population.

In addition to the warm trapped electrons described above, the plug contains hot electrons passing from the barrier and cold electrons passing from the central cell whose densities n_{eha} and n_{eca}, respectively, are calculated in the Appendix.

The plug beta parameter is given by

$$\beta_a = \frac{0.9\, n_{iha} E_{iha} + n_{ewa} T_{ew} + n_{eca} T_{ec} + 0.8\, n_{eha} E_{eh}}{2.5 \times 10^7\, B_a^2} , \tag{43}$$

where the factors 0.9 and 0.8 in the sloshing ion and hot electron pressures account for the anisotropy of their respective distribution functions [3]. B_a is the vacuum magnetic field at the plug point.

The plug ambipolar potential ϕ_c and warm electron density n_{ewa} are obtained by solving the system of equations formed by the ambipolarity condition at the plug

$$V_a \frac{dn_{ewa}}{dt} = V_{ih} \frac{dn_{iha}}{dt} , \tag{44}$$

together with the quasineutrality condition

$$n_{iha} = n_{ewa} + n_{eca} + n_{eha} . \tag{45}$$

The time derivatives dn_{ewa}/dt and dn_{iha}/dt are given by Eqs. (40) and (35), respectively, and n_{iha} is obtained by integration of Eq. (35).

2.5 Global Ambipolarity

An equation is necessary to obtain the central cell electron confinement potential ϕ_e. We use the condition of plasma global ambipolarity

$$\sum_i \left(z_i V_i \frac{dn_i}{dt}\right) = \sum_e \left(V_e \frac{dn_e}{dt}\right) \tag{46}$$

where the subscripts i and e stand for all the trapped ion and electron species which are considered in the device, and z_i is the ion atomic number. Substituting Eqs. (3), (6), (9), (11), (17), (23), (28), (35), and (40) into Eq. (46), we obtain

$$\left[\frac{n_{ic}^2}{(n\tau)_{ic}} + \frac{1}{2} n_{ic}^2 \langle\sigma V\rangle_{dt} (1 - f_{\alpha t}) + 2C_{\alpha\ell} n_{c\alpha}\right] V_c + \frac{n_{iha}^2}{(n\tau)_{iha}} 2V_{ih} = \frac{n_{ec}^2}{(n\tau)_{ec}} V_c \,. \tag{47}$$

This equation gives the net charge variation in the machine. It contains end losses of central cell ions, electrons, and sloshing ions and terms related with alpha particle production and loss. Equation (47) is solved for the electron confinement potential, ϕ_e.

We comment next about the methods employed in the preceding sections to obtain the ambipolar potentials in the various regions along the axis of the device. The quasineutrality condition $\sum_e n_e = \sum_i z_i n_i$ is satisfied everywhere. This condition is established in a very short time of the order of the bounce time, τ_b. To maintain a quasineutral plasma, the particle flux through the boundary of every region needs to be ambipolar. Ambipolarity only concerns the trapped species because, in the limit $\tau_b \to 0$, passing particles enter and leave the region instantaneously. In a time dependent analysis as the one considered here, the time scale for variation in the electron distribution

function is much shorter than the characteristic time for variation of the ion distribution function. It is because of this reason that during typical time intervals for integration of the ion equations we consider the electron distribution as varying on a finer time scale as to preserve ambipolarity and quasineutrality along the axis of the device. For a given ion density in a space region, these two constraints determine the electron trapped density and the ambipolar potential. In this sense the dynamics of the plasma can be viewed as a series of instantaneous calculations in which a consistent set of ambipolarity and quasineutrality conditions are solved, linked by the integration in time of the density of the trapped ion species.

2.6 Energy Multiplication Factor

The energy multiplication factor Q is defined as the ratio of the fusion power to the total external absorbed power. The fusion power is defined as the power carried out by neutrons produced in the fusion reactions,

$$P_{fus} = \frac{n_{ic}^2}{4} \langle \sigma V \rangle_{dt} E_{nf} V_c \ , \tag{48}$$

where $\langle \sigma V \rangle_{dt}$ is the fusion cross section for central cell ions, E_{nf} is the energy of the neutrons produced per fusion event (14 MeV) and V_c is the effective central cell volume. Only fusion power produced in the central cell is taken into account. The total absorbed power includes contributions from the central cell neutral beam, gas, ICRH and RF electron heating; axicell neutral beam; transition and barrier pumping neutral beams; sloshing ion beam; and RF power applied at the barrier and plug.

Only a fraction of the power absorbed by the plasma actually results in an increase in the plasma thermal energy. The remaining absorbed power is

spent either to counteract for the various loss mechanisms or to provide the potential energy required by particles moving along the machine. The loss mechanisms include ion and electron end losses, synchrotron radiation and power carried out by the neutrals produced by charge exchange reactions off the various neutral beams injected in the plasma. A part of the end losses can be recovered by direct conversion. Neutrals produced by charge exchange reactions end up heating the wall of the device. A fraction of the power deposited there can also be recovered by the thermal cycle. Alpha particles born in fusion reactions provide a heating source to the plasma.

To obtain the neutral beam injected power, the absorbed power is divided by the neutral beam trapping fractions given by [15]

$$f_{tr} = 1 - \exp\left(- \frac{4.52 \times 10^{-8}\, n\ell \langle\sigma V\rangle_{tot}}{(E_{nb}/A_{nb})^{1/2}}\right) ,$$

where n is the total density, ℓ is the path length, $\langle\sigma V\rangle_{tot}$ is the total cross section including all reactions that cause beam attenuation, E_{nb} is the injection energy and A_{nb} is the neutral mass number.

3. MFTF-B STARTUP SCENARIO

The tandem mirror model described in Section 2 has been solved numerically. The density and temperature rate equations form a system of ordinary differential equations that are integrated to obtain the time evolution of density and temperature of each species for given variable sources injected into the plasma. Initial conditions are provided by the target plasma. Ambipolar potentials are calculated at each timestep by solving a system of nonlinear equations. To integrate the rate equations a predictor-corrector method is

used. The predictor is Euler's formula and the corrector uses a quadratic form. The timestep length is limited to 10% of the shortest characteristic time for density or temperature variations. The set of densities and temperatures obtained as a result of the time integration may be such that the nonlinear system of equations that gives the ambipolar potentials either does not have roots or the roots are not within the physically feasible ranges. The conditions for the potential equations to have roots and the criteria followed in the code to choose one of the roots when there are more than one, are explained in detail in Ref. [16]. The basic idea has been to choose those roots which imply physically meaningful solutions. The numerical code developed to solve the physics model is used to evaluate startup scenarios for barrier tandem mirror configurations. The code can also be used in studying near steady state situations and make parametric studies to evaluate different designs. Plasma startup has to be accomplished while minimizing the amount of injected power and particle sources. An ideal case would be to reach the stationary operating point using only the power supplies needed at steady state operation, but in general this is not the case. In order to reach a steady state operating point, a tandem mirror plasma needs to be fed with a variety of carefully programmed sources.

A number of constraints on the plasma parameters must be satisfied at all times during operation in order for the plasma to be maintained. Some constraints are related to the stability criteria for the most dangerous modes relevant to the tandem mirror configuration. The tandem mirror configuration is an average minimum-B system. MHD stability is provided by building up the plasma pressure in the regions with good magnetic field curvature (anchors) above the plasma pressure of the regions with neutral or bad magnetic field

curvature. Microstability of the plug plasma is provided by ions streaming out from the central cell and is substantially enhanced by the sloshing character of the hot ions as well as by the mirror confined electrons. To be stable, the plug plasma must exceed a minimum ratio of the cold ion density to hot ion density in the midplane of the plugs. Thus, microstability is ensured when the cold ions start to be electrostatically confined. Microstability of the central cell plasma will be provided by the electrostatic confinement of low energy ions. Stability to trapped particle modes requires maintaining an adequate ratio of plug passing ions to central cell ions. Therefore, the plasma will be less susceptible to trapped particle modes if the plug potential buildup starts before thermal barrier formation. These issues are discussed in detail in Ref. [2].

We present a possible scenario for the startup of the axicell MFTF-B reference case (MARS mode) [2]. Table 1 shows the machine parameters and the initial conditions. The startup scenario discussed here is based on the startup scenario proposed for the TMX-Upgrade with thermal barriers [17]. In this scenario every cell is started simultaneously. An initial plasma is created either by plasma guns or by RF ionization of gas. Then all systems are turned on except for the transition and barrier pump beams which will be connected at a later time as needed. During the early stages of its buildup, the central cell is fueled by gas and heated by ICRH. This kind of heating has been shown [17] to be more efficient at low densities than the heating by neutral beams. Sloshing ion neutral beams (80 keV) are used to provide microstability and MHD stability and also to help in the formation of the plug potential. ECRH applied at the barrier heats the mirror confined electrons. Additional RF heating applied at the plug heats the warm plug electrons. As

the efficiency of gas as a central cell fuel starts to decrease due to the increase of temperature, another system should be provided to continue the buildup of the central cell density. We have chosen 80 keV neutral beams. Pellet injection would be an alternative form of central cell fueling. The axicell neutral beam (70 keV) can be connected at any time as needed. This neutral beam creates a potential bump which confines low energy central cell ions while the outer confining potential peak is formed. Transition and barrier pump beams are turned on when the accumulation of central cell ions trapped in the transition and barrier regions cause a reduction on the respective potential dips. Their energies are 40 keV and 80 keV, respectively. The transition region neutral beam is also used to control the plasma pressure in that region.

The startup scenario described here lasts approximately 1.5 seconds. Figures 5.a to 5.ℓ show in detail the time evolution of the plasma parameters as well as the injected sources that are absorbed in the plasma. The initial values of the central cell gas source (40 A), sloshing ion source (12 A), central cell ICRF power (1.2 MW), barrier RF power (0.2 MW) and plug RF power (0.1 MW) are such that they allow the plasma buildup to proceed at the desired rate. Successive changes in the source levels are imposed when the injected sources are no longer appropriate to sustain the plasma buildup. By varying the central cell gas, neutral beam and ICRH it is possible to find a combination that provides the amount of particles and energy required for central cell buildup.

Figure 5.a presents the time evolution of the plasma temperatures. The species sustained by neutral beams (axicell hot ions and sloshing ions) reach their steady state mean energy in a few milliseconds. Central cell ions are

fueled by cold gas and heated by ICRH. In order to maintain the ICRH power within reasonable limits ion temperature buildup has to proceed at a slow rate. At time ≃ 0.35 s the central cell density buildup requires an increase of particle fueling which is provided by an increase in the gas injection rate as well as by turning on the central cell neutral beam. ICRH is reduced at the same time. The combined effects of these changes are reflected in the central cell ion temperature evolution. The temperature of the anchor electron species is very difficult to control for small changes in the RF power applied at the barrier and plug cause large variations in the warm and hot electron temperatures.

Figures 5.b and 5.c show the time evolution of the density of the various plasma species. In this scenario, the buildup of the axicell hot ions starts at time zero to help in the confinement of central cell ions. At time ~ 0.35 s, the growth rate of the central cell ion density starts to decrease and the central cell sources are adjusted (see Figs. 5.h to 5.i). The central cell alpha particle density is calculated assuming a DT-mixture fuel. MFTF-B is an experiment designed to use deuterium fuel. DT fuel has been used in this simulation to evaluate the energy multiplication factor Q. It is assumed here that alpha particles are confined in the central cell.

Figure 5.d shows the time evolution of the radially averaged beta parameter in every region of the device. The barrier and plug plasma pressures provide MHD stability for the system. Figure 5.e shows the ambipolar potentials. Figure 5.f shows the time evolution of the confinement products ($n\tau$). The behavior of the central cell ion and electron confinement products depend on the potential to temperature ratio. At the initial stages of the startup the central cell confinement potentials grow faster than the tempera-

tures and the opposite is true as steady state is approached. The sloshing ion confinement product decreases logarithmically with the plug potential. Figure 5.g shows the time evolution of the transition and barrier pumping parameters as well as the transition and barrier trapping rates. Their variation with time is closely related to the variation of the central cell ion temperature.

Figures 5.h to 5.k show the particle and energy sources required for the startup scenario proposed. The axicell, transition and barrier particle sources are presented in Fig. 5.h. Curves 1 and 2 give the neutral injection rate and the neutral absorption rate due to the axicell neutral beam, respectively. Curves 3 and 4 give, respectively, the neutral injection rate and the neutral absorption rate provided by the transition region pumping neutral beam. The beam is turned on at time $\simeq$ 0.5 s. Curves 5 and 6 give the neutral injection rate and neutral absorption rate due to the barrier pumping neutral beam, respectively. The barrier beam is turned on at time $\simeq$ 0.9 s.

Figure 5.i shows the sloshing ion and central cell particle sources. Curves 1 and 2 give the neutral injection and absorption rate of the sloshing ion neutral beam, respectively. Curves 3 and 4 give the injection and absorption rates of the central cell neutral beam. Curves 5 and 6 describe the central cell fueling by gas and its ionization rate, respectively. The absorption fraction of the gas is taken to be unity. The efficiency of fueling by gas, unlike fueling by neutral beams, decreases as plasma buildup progresses. At time $\simeq$ 0.35 s, the gas injection rate is increased to 60 A, and the central cell neutral beam is turned on. At the same time the ICRH heating is reduced. At time $\simeq$ 0.5 s the gas and ICRH are gradually turned off while the central cell neutral beam takes over central cell fueling and heating.

Figure 5.j shows the neutral beam power injected in the plasma. Figure 5.k shows the time evolution of the RF power injected and absorbed in the plasma: auxiliary central cell ion heating, plug electron heating and barrier electron heating. The absorption of RF power by the plasma depends on the specific launching structure used. The power levels shown in Fig. 5.k are normalized assuming total absorption at steady state. The RF power absorbed is calculated assuming that the absorption fraction is proportional to the density. When the central cell neutral beam is connected, ICRH power is gradually turned off. Finally, in Fig. 5.l, curve 1 shows the fusion power produced in the central cell assuming a DT-mixture fuel. Curves 2 and 3 show the total power injected and absorbed in the plasma, respectively, and Curve 4 gives the equivalent energy multiplication factor for a D-T mixture fuel.

4. CONCLUSION

We have analyzed the time evolution of a plasma confined in a tandem mirror with thermal barriers. We have presented a time dependent physics model that describes the kinetic interactions in velocity space of the various plasma species that exist in each spatial region of the confinement and the effect of a variety of particle and energy sources applied to the plasma. The configuration considered in this study is the axicell MFTF-B [2,3] reference case.

The physics model includes particle and energy rate equations for the various species that determine the plasma confinement and quasineutrality and ambipolarity conditions which define the ambipolar potential profile along the axis of the device. Expressions to obtain the passing particle densities are also included. The region-averaged properties of each plasma species are calculated. The particle and energy rate equations have been written utili-

zing the available analytical and numerical results of kinetic problems in tandem mirror devices. The model describes in a self-consistent manner the time evolution of tandem mirror confinement with thermal barriers including the steady state phase of operation. The physics model is solved numerically. The equations describing the time variation of densities and temperatures of the various species form a system of differential equations coupled by the equations which determine the ambipolar potential in the different regions. The calculation of the ambipolar potentials requires finding a physically valid solution to a system of nonlinear equations at each timestep. In order to obtain a complete startup time sequence the particle and energy sources applied to the plasma need to be carefully programmed. In addition, a reasonable startup scenario should minimize the intensity of the sources required to achieve plasma buildup, and should satisfy at all times the stability criteria for the plasma. Following these ideas we have obtained a startup scenario for the axicell MFTF-B. We have given the sequence of particle and energy sources that are required for plasma buildup starting from a target plasma.

The numerical code can also be used to make parametric studies near steady state in order to evaluate different design points of a configuration. This approach to solve the problem of startup of barrier tandem mirrors has the benefit of allowing the consideration of detailed particle interactions in an economical way as well as to make fast evaluations of possible startup scenarios and find the power and particle sources required for the plasma to evolve from a given initial state to the stationary operating point. An important advantage of this approach is its self-consistency. To properly solve the problem, all species that exist at every region need to be taken into account.

Because of the passing species, all spatial regions of the device are closely interrelated and the effects of an external action over any of the regions affects the entire structure of the confinement. Simple calculations that simulate the variation of some regions or species while maintaining the rest constant are not meaningful due to the lack of self-consistency.

APPENDIX: PASSING PARTICLE DENSITIES

The passing densities at various locations along the axis for the axicell MFTF-B [2,3] are calculated using the relation that equates the distribution function expressed in terms of the particle constants of motion at different points along field lines. This condition is correct to lowest order in the ratio of collision frequency to bounce frequency. We assume local Maxwellian distribution functions for the trapped particles.

The ion velocity space in E, μ variables is shown in Fig. 2. Central cell ions occupy the velocity space domain located above the line $E = \mu B_c$, except for the central cell loss cone region. The central cell potential is taken as the reference potential.

Central cell passing ions at the axicell midplane, point "x", occupy the regions labeled I, II and III in Fig. 2. We will include also as part of the passing region the central cell loss cone. This can be justified by noticing that the axicell outboard magnetic peak which provides magnetic confinement to the central cell particles is located outside of the point "x" and, therefore, the approximation of including the loss region as a part of the passing region at "x" has a small effect on the passing ion density at "x".

The passing ion density at the axicell midplane is then given by,

$$n_{icx} = n_{ic} \exp\left(-\frac{\phi_x}{T_{ic}}\right)\left[1 - (1 - R_{x,xi})^{1/2} \exp\left(\frac{\phi_x R_{x,xi}}{T_{ic}(R_{x,xi} - 1)}\right)\right] .$$

Central cell ions passing through the axicell outboard peak, point "xo", occupy the region labeled I in Fig. 2. For particles at "xo" and farther along the axis, the effect of the central cell loss cone on the passing ion density calculation becomes increasingly important as the point in which the passing density is calculated moves towards the ends of the device. For the axicell MFTF-B parameters the central cell loss cone correction to the passing density at "xo" is ~ 50%. Thus, the passing ion region does not include the central cell loss cone. The passing ion density at the axicell outboard peak is given by

$$n_{ipxo} = 0$$

for $\phi_c < \phi_x$. For $E^+ > E'$ (see Fig. 2)

$$n_{ipxo} = n_{ic} \exp\left(-\frac{\phi_x}{T_{ic}}\right)\left[\exp(x)\left(\operatorname{erfc}\sqrt{x} - \operatorname{erfc}\sqrt{x + x_c}\right) + (R_{xo,a} - 1)^{1/2} \frac{2}{\sqrt{\pi}}\right.$$

$$\left.*\left(\exp\left(-\frac{x_c R_{x,a}}{(R_{x,a} - 1)}\right) D\sqrt{-\frac{x_c R_{x,a}}{(R_{x,a} - 1)} \frac{1 - R_{xo,x}}{1 - R_{xo,a}} - \frac{x}{(1 - R_{xo,a})}}\right)\right.$$

$$\left. - \exp(-x_c)\, D\sqrt{\frac{x + x_c}{R_{xo,a} - 1}}\right) - (R_{xo,x} - 1)^{1/2} \frac{2}{\sqrt{\pi}} \left(\exp\left(-\frac{x_c R_{x,a}}{(R_{x,a} - 1)}\right)\right.$$

$$* D\sqrt{-\frac{x_c R_{x,a}}{R_{x,a} - 1} - \frac{x}{(1 - R_{xo,x})}} - D\sqrt{\frac{x}{R_{xo,x} - 1}}\,)]\ ,$$

where $$x = \frac{\phi_{xo}}{T_{ic}}$$

$$x_c = \frac{\phi_c - \phi_x}{T_{ic}}$$

and $$D(z) = e^{-z^2} \int_0^z e^{z^2}\, dz$$

in Dawson's integral.

For $(E^+ < E')$,

$$n_{ipxo} = n_{ic} \exp(-\frac{\phi_x}{T_{ic}})[\exp(x)\ \mathrm{erfc}\sqrt{x} + \frac{2}{\sqrt{\pi}} (R_{xo,x} - 1)^{1/2} D\sqrt{\frac{x}{R_{xo,x} - 1}}$$

$$- \exp(x)\ \mathrm{erfc}\sqrt{x + x_c} - \frac{2}{\sqrt{\pi}} (R_{xo,a} - 1)^{1/2} \exp(-x_c)\ D\sqrt{\frac{x + x_c}{R_{xo,a} - 1}}\ ]\ .$$

Next, we calculate the central cell ion passing density at points beyond the axicell outboard peak: transition t, yin-yang inboard peak y_i, sloshing ion inside peak a' and barrier midplane b. The passing region is labeled I in Fig. 2. These points have the same type of expression for their passing density. We evaluate the passing density at a point with magnetic field B_j and relative potential $\phi_x - \phi_j$ with respect to the central cell. The passing ion density at the point j is as follows.

For $\phi_c < \phi_x$

$$n_{ipj} = 0 \ .$$

For $\phi_c > \phi_x$

$$n_{ipj} = n_{ic} \exp(-\frac{\phi_c}{T_{ic}})[\exp(x) \ \mathrm{erfc}\sqrt{x} - \sqrt{1 - R_{j,xo}} \exp(x_{jo}) \ \mathrm{erfc}\sqrt{x_{jo} + x_{xo}}$$

$$- \sqrt{1 - R_{j,x}} \ (\exp(x_j) \ \mathrm{erfc}\sqrt{x_j} - \exp(x_j) \ \mathrm{erfc}\sqrt{x_j + x_{xo}})] - n_{\ell cj} \ ,$$

where

$$x = \frac{\phi_j}{T_{ic}} \ ,$$

$$x_j = \frac{\phi_j}{T_{ic}(1 - R_{j,x})} \ ,$$

$$x_{jo} = \frac{\phi_j - \phi_{xo} R_{j,xo}}{T_{ic}(1 - R_{j,xo})} \ ,$$

$$x_{xo} = \frac{\phi_{xo}}{T_{ic}(R_{xo,x} - 1)} \ ,$$

and the loss cone contribution $n_{\ell cj}$ is given next.

First we consider the case $R_{j,a} = B_j/B_a < 1$. For $\phi_c < \phi_x + \phi_{xo}(R_{x,a} - 1)/(R_{xo,a} - R_{x,a})$,

$$n_{\ell cj} = n_{ic} \exp\left(-\frac{\phi_x}{T_{ic}}\right)\left[\exp(x)\ \mathrm{erfc}\sqrt{x + x_c} - (1 - R_{j,a})^{1/2} \exp(x_{aj} + x_{cj}R_{j,a})\right.$$

$$\left.*\left(\mathrm{erfc}\sqrt{x_{cj} + x_{aj}} - \mathrm{erfc}\sqrt{\frac{x_c}{(R_{x,a} - 1)} + x_{aj} + x_{cj}}\right)\right.$$

$$\left. - (1 - R_{j,x})^{1/2} \exp(x_j)\left(\mathrm{erfc}\sqrt{\frac{x_c}{R_{x,a} - 1}\frac{1 - R_{j,a}}{1 - R_{j,x}} + x_j + \frac{x_c}{(1 - R_{j,x})}}\right.\right.$$

$$\left.\left. - \mathrm{erfc}\sqrt{x_{xo} + x_j}\right) - (1 - R_{j,xo})^{1/2} \exp(x_{jo})\ \mathrm{erfc}\sqrt{x_{xo} + x_{jo}}\ \right] ,$$

where

$$x_c = \frac{\phi_c - \phi_x}{T_{ic}} ,$$

$$x_{cj} = \frac{\phi_c - \phi_x}{T_{ic}(1 - R_{j,a})} ,$$

$$x_{aj} = \frac{\phi_j}{T_{ic}(1 - R_{j,a})} .$$

For $\phi_c > \phi_x + \phi_{xo}(R_{x,a} - 1)/(R_{xo,a} - R_{x,a})$,

$$n_{\ell cj} = n_{ic} \exp\left(-\frac{\phi_x}{T_{ic}}\right)\left[\exp(x)\ \mathrm{erfc}\sqrt{x + x_c} - (1 - R_{j,a})^{1/2} \exp(x_{aj} + x_{cj}R_{j,a})\right.$$

$$\left.*\left(\mathrm{erfc}\sqrt{x_{cj} + x_{aj}} + \mathrm{erfc}\sqrt{x_{cj} + x_{aj} + x_{ao} + x_{co}}\right)\right.$$

$$\left. - (1 - R_{j,xo})^{1/2} \exp(x_{jo})\ \mathrm{erfc}\sqrt{x_{jo} + x_{co}R_{xo,a} + x_{ao}}\ \right] ,$$

where $$x_{ao} = \frac{\phi_{xo}}{R_{xo,a} - 1} ,$$

and $$x_{co} = \frac{\phi_c - \phi_x}{R_{xo,a} - 1} .$$

Next we consider the case $R_{j,a} = B_j/B_a > 1$. For $\phi_c < \phi_x + \phi_{xo}(R_{x,a} - 1)/(R_{xo,a} - R_{x,a})$,

$$n_{\ell cj} = n_{ic} \exp(-\frac{\phi_x}{T_{ic}})[\exp(x) \operatorname{erfc}\sqrt{x + x_c} + (R_{j,a} - 1)^{1/2} \frac{2}{\sqrt{\pi}}$$

$$*(\exp(-x_c) D\sqrt{-(x_{cj} + x_{aj})} - \exp(-x_{ca}R_{xa}) D\sqrt{-x_{ca} - x_{cj} - x_{aj}})$$

$$- (1 - R_{j,x})^{1/2} \exp(x_j)(\operatorname{erfc} \sqrt{x_{ca} \frac{(1 - R_{j,a})}{(1 - R_{j,x})} + x_{cj} + x_{aj}}$$

$$- \operatorname{erfc}\sqrt{x_{xo} + x_j}) - (1 - R_{j,xo})^{1/2} \exp(x_{jo}) \operatorname{erfc}\sqrt{x_{xo} + x_{jo}}] ,$$

where $$x_{ca} = \frac{\phi_c - \phi_x}{R_{x,a} - 1} .$$

For $\phi_c > \phi_x + \phi_{xo}(R_{x,a} - 1)/(R_{xo,a} - R_{x,a})$

$$n_{\ell cj} = n_{ic} \exp(-\frac{\phi_x}{T_{ic}})[\exp(x) \operatorname{erfc}\sqrt{x + x_c} - (R_{j,a} - 1)^{1/2} \frac{2}{\sqrt{\pi}} [\exp(-x_{co}R_{xo,a}$$

$$- x_{ao}) D\sqrt{-x_{cj} - x_{aj} - x_{ao} - x_{co}} + \exp(-x_c) D\sqrt{-x_{cj} - x_{aj}}]$$

$$- (1 - R_{j,xo})^{1/2} \exp(x_{jo}) \operatorname{erfc}\sqrt{x_{jo} + x_{xo}R_{xo,a} + x_{ao}}] .$$

The electron velocity space in E, μ variables is shown in Fig. 3. Central cell electrons occupy the region located above the line $E = \mu B_c$, except for the central cell loss cone. Electrons passing through the axicell outboard magnetic field peak and beyond, occupy the region located to the left of $E = \mu B_{xo} + (\phi_{xo} - \phi_x)$. Three electron species are considered: central cell electrons (cold), plug electrons (warm) and hot, barrier electrons. Warm and hot electrons are confined to the anchor. We assume that the rest of the device contains only central cell passing electrons. Figure 3 shows the warm and hot regions; the remaining space is considered the cold region. To calculate the cold electron density along the machine a central cell Maxwellian distribution function is assumed. The cold electron density at the axicell midplane "x", neglecting the loss cone effect, is given by

$$n_{ecx} = n_{ec} \exp\left(\frac{\phi_c}{T_{ec}}\right)$$

where n_{ec} and T_{ec} are the central cell electron density and temperature. Similarly, at the axicell outboard peak "xo", the cold electron density is given by

$$n_{exco} = n_{ec} \exp\left(\frac{\phi_x - \phi_{xo}}{T_{ec}}\right) ,$$

where the loss cone effect has been neglected.

For points located outside the axicell, the loss region becomes broader and its effect on the cold density is significant. The cold electron density at the transition is given by

$$n_{ect} = n_{ec} \exp\left(\frac{\phi_x - \phi_t}{T_{ec}}\right)\left[1 - \operatorname{erfc}\sqrt{\frac{\phi_e - \phi_t + \phi_x}{T_{ec}}} + (1 - R_{t,yo})^{1/2}\right.$$

$$\left. * \operatorname{erfc}\sqrt{\frac{\phi_e - \phi_t + \phi_x}{T_{ec}(1 - R_{t,yo})}} \exp\left(\frac{R_{t,yo}(\phi_e - \phi_t + \phi_x)}{T_{ec}(1 - R_{t,yo})}\right)\right] .$$

The same expression holds for the inboard yin-yang peak "yi" after substituting ϕ_t by ϕ_{yi} and B_t by B_{yi}, and assuming $B_{yi} < B_{yo}$.

Next we consider the anchor region where at every point there is more than one electron species. At the inboard sloshing ion density peak, point "a'", we have two species. Cold electrons are located above the line $E = \mu B_{yi} + (\phi_{yi} - \phi_x)$ and their upper energy limit is the loss region boundary. Hot electrons are bounded by the lines $E = \mu B_{yi} + \phi_{yi} - \phi_x$ and $E = \mu B_{a'} + \phi_{a'} - \phi_x$. The cold electron density at a' is

$$n_{eca'} = n_{ec} \exp\left(\frac{\phi_x - \phi_{a'}}{T_{ec}}\right)\left[\operatorname{erfc}\sqrt{\frac{\phi_{yi} - \phi_{a'}}{T_{ec}}} - \operatorname{erfc}\sqrt{\frac{\phi_e - \phi_a + \phi_x}{T_{ec}}}\right.$$

$$- (1 - R_{a',yi})^{1/2} \operatorname{erfc}\sqrt{\frac{\phi_{yi} - \phi_{a'}}{T_{ec}(1 - R_{a',yi})}} \exp\left(\frac{R_{a',yi}(\phi_{yi} - \phi_{a'})}{T_{ec}(1 - R_{a',yi})}\right)$$

$$\left. + (1 - R_{a',yo})^{1/2} \operatorname{erfc}\sqrt{\frac{\phi_e - \phi_{a'} + \phi_x}{T_{ec}(1 - R_{a',yo})}} \exp\left(\frac{R_{a',yi}(\phi_e - \phi_{a'} + \phi_x)}{T_{ec}(1 - R_{a',yo})}\right)\right] .$$

Barrier electrons are located above the line $E = \mu B_b + \phi_b - \phi_x$ (Fig. 3). Those located to the left of $E = \mu B_{yi} + \phi_{yi} - \phi_x$ are the cold species. The rest of them are hot, barrier electrons. The upper boundary for the cold species is the loss region. The cold electron density at the barrier is given

by

$$n_{ecb} = n_{ec} \exp\left(\frac{\phi_x - \phi_b}{T_{ec}}\right)\left[1 - (1 - R_{b,yi})^{1/2} \exp\left(\frac{R_{b,yi}(\phi_{yi} - \phi_b)}{T_{ec}(1 - R_{b,yi})}\right)\right.$$

$$- \operatorname{erfc}\sqrt{\frac{\phi_e - \phi_b + \phi_x}{T_{ec}}} + (1 - R_{b,yo})^{1/2} \operatorname{erfc}\sqrt{\frac{\phi_e - \phi_b + \phi_x}{T_{ec}(1 - R_{b,yo})}}$$

$$\left. * \exp\left(\frac{R_{b,yo}(\phi_e - \phi_b - \phi_x)}{T_{ec}(1 - R_{b,yo})}\right)\right] .$$

In the plug region there are three electron species. Warm electrons are confined to the plug. Cold electrons are situated above the barrier base energy line $E = \mu B_b + \phi_b - \phi_x$, to the left of $E = \mu B_{yi} + \phi_{yi} - \phi_x$. Hot electrons are located above the line $E = \mu B_b + \phi_b - \phi_x$ and to the right of $E = \mu B_{yi} + \phi_{yi} - \phi_x$. The upper boundary of the cold region is the loss cone. The cold electron density at the plug is given by

$$n_{eca} = n_{ec} \exp\left(\frac{\phi_x - \phi_b}{T_{ec}}\right)\left[\exp\left(\frac{\phi_a}{T_{ec}}\right) \operatorname{erfc}\sqrt{\frac{\phi_a}{T_{ec}}} + \frac{2}{\sqrt{\pi}} (R_{a,b} - 1)^{1/2}\right.$$

$$* \left(D\sqrt{\frac{\phi_a}{T_{ec}(R_{a,b} - 1)}} - \exp\left(-\frac{\phi_b - \phi_{yi}}{(R_{yi,b} - 1)T_{ec}}\right)\right.$$

$$\left. \left. * D\sqrt{\frac{\phi_b - \phi_{yi}}{T_{ec}(1 - R_{yi,b})} + \frac{\phi_a}{T_{ec}(R_{a,b} - 1)}}\right) - (1 - R_{a,yi})^{1/2}\right.$$

$$* \exp\left(\frac{\phi_a - (\phi_b - \phi_{yi})R_{a,yi}}{T_{ec}(1 - R_{a,yi})}\right) \operatorname{erfc}\sqrt{\frac{(\phi_b - \phi_{yi})(1 - R_{a,b}) + \phi_a(R_{yi,b} - 1)}{T_{ec}(R_{yi,b} - 1)(1 - R_{a,yi})}}$$

$$- \exp\left(\frac{\phi_a}{T_{ec}}\right) \operatorname{erfc}\sqrt{\frac{\phi_c + \phi_e}{T_{ec}}} + (1 - R_{a,yo})^{1/2} \operatorname{erfc}\sqrt{\frac{\phi_c + \phi_e}{T_{ec}(1 - R_{a,yo})}}$$

$$* \exp\left(\frac{\phi_a}{T_{ec}} + \frac{\phi_c + \phi_e}{T_{ec}(R_{yo,a} - 1)}\right)] \ .$$

The barrier hot electron population is centered at the barrier midplane. Its density falls to zero at the inboard and outboard yin-yang peaks. We assume a Maxwellian distribution function for the barrier hot electrons, with $T_{eb} = 0.8\ E_{ehb}$, neglecting the anisotropy of the actual distribution function. The hot electron region at the inboard sloshing ion peak, point a', is the part of velocity space limited by the lines $E = \mu B_{a'} + \phi_{a'} - \phi_x$ and $E = \mu B_{yi} + \phi_{yi} - \phi_x$. The hot electron density at a' is then given by

$$n_{eha'} = n_{ehb} A_o \exp\left(\frac{\phi_b - \phi_{a'}}{T_{eb}}\right)[1 + (1 - R_{a',yi})^{1/2} \exp\left(\frac{R_{a',yi}(\phi_{yi} - \phi_{a'})}{T_{eb}(1 - R_{a',yi})}\right)$$

$$* \operatorname{erfc}\sqrt{\frac{\phi_{yi} - \phi_{a'}}{T_{eb}(1 - R_{a',yi})}} - \operatorname{erfc}\sqrt{\frac{\phi_{yi} - \phi_{a'}}{T_{ec}}}\ ] \ ,$$

where $$A_o^{-1} = (1 - R_{b,yi})^{1/2} \exp\left(\frac{(\phi_{yi} - \phi_b)R_{b,yi}}{T_{eb}(1 - R_{b,yi})}\right) \ .$$

The plug hot electron region D_1, is located above the line $E = \mu B_b + \phi_b - \phi_x$ and to the right of the line $E = \mu B_{yi} + \phi_{yi} - \phi_x$. The hot electron density at the plug is given by

$$n_{eha} = n_{ehb} A_o \exp\left(\frac{\phi_b + \phi_c - \phi_x}{T_{eb}}\right)\left[(1 - R_{a,yi})^{1/2} \exp\left(\frac{R_{a,yi}(\phi_c + \phi_{yi} - \phi_x)}{T_{eb}(1 - R_{a,yi})}\right)\right.$$

$$* \operatorname{erfc}\sqrt{\frac{(\phi_b - \phi_{yi})R_{yi,b}}{T_{eb}(1 - R_{yi,b})} + \frac{\phi_{yi} - \phi_x + \phi_c}{T_{eb}(1 - R_{a,yi})}}$$

$$+ (R_{a,b} - 1)^{1/2} \exp\left(\frac{\phi_{yi} - \phi_b}{T_{eb}(R_{yi,b} - 1)} - \frac{\phi_b + \phi_c - \phi_x}{T_{eb}}\right) \frac{2}{\sqrt{\pi}}$$

$$\left. * D\sqrt{\frac{\phi_{yi} - \phi_b}{T_{eb}(R_{yi,b} - 1)} - \frac{\phi_b + \phi_c - \phi_x}{T_{eb}(1 - R_{a,b})}}\right] .$$

ACKNOWLEDGEMENTS

We wish to thank John Santarius and R. Carrera for helpful conversations. This work has been supported by the U.S. Department of Energy.

REFERENCES

1. Baldwin, D.E., Logan, B.G., Phys. Rev. Lett. 43 (1979) 1318.

2. Thomassen, K.I., Karpenko, V.N., "An Axicell Design for the End Plugs of MFTF-B," Lawrence Livermore Laboratory Report UCID-19318 (1982).

3. Baldwin, D.E., Logan, B.G., (Eds.), "Physics Basis for an Axicell Design of the End Plug of MFTF-B," Lawrence Livermore Laboratory Report UCID-19359 (1982).

4. Pastukhov, V.P., Nucl. Fusion 14 (1974) 3.

5. Rensink, M.E., Mirin, A.A., Tomaschke, G.P., Bull. Am. Phys. Soc. 26 (1981) 1007.

6. Sivukhin, D.V., in Reviews of Plasma Physics, edited by M.A. Leontovich, 4 (1966) 93.

7. Rognlien, T.D., Cutler, T.A., Nucl. Fusion 20 (1980) 1003.

8. Logan, B.G., Mirin, A.A., Rensink, M.E., Nucl. Fusion 20 (1980) 1613.

9. Carlson, G.A., Arfin, B., Barr, W.L., Boghosian, B.M., Erickson, J.L., "Tandem Mirror Reactor with Thermal Barriers," Lawrence Livermore National Laboratory Report UCID-52836 (1979).

10. Book, D.L., NRL Plasma Formulary (1980).

11. Carrera, R., Catto, P.J., Phys. Fluids 28 (1985) 1906.

12. Baldwin, D.E., Logan, B.G., Simonen, T.C., (Eds.), "Physics Basis for MFTF-B," Lawrence Livermore National Laboratory Report UCID-18496 (1980).

13. Gilmore, J.M., "Build Up of the Central Cell Plasma in a Tandem Mirror," Ph.D. Thesis, University of Wisconsin (1980).

14. Trubnikov, B.A., ZhEtf Pis. Red 16 (1972) 37.

15. Riviere, A.C., Nucl. Fusion 11 (1971) 363.

16. Montalvo, E., "Time Dependent Studies of a Tandem Mirror with Thermal Barriers," Ph.D. Thesis, University of Wisconsin (1983).

17. Molvik, A.W., Falebella, S., "Use of ICRH for Startup and Initial Heating of the TMX-U Central Cell," Lawrence Livermore National Laboratory Report UCID-19342 (1982).

Table 1. MFTF-B parameters and Initial Conditions

Magnetic Fields (T)

$B_c = 1.0$
$B_{xi} = 6.0$
$B_x = 4.0$
$B_{xo} = 12.0$
$B_t = 0.85$
$B_{yi} = 3.0$
$B_b = 1.0$
$B_a = 1.4$
$B_{yo} = 3.0$

Dimensions (cm)

$L_{eff,c} = 1260.0$
$L_{eff,x} = 51.3$
$L_{eff,t} = 723.0$
$L_{eff,b} = 145.0$
$L_{eff,a} = 145.0$
$L_{eff,eh} = 184.0$
$L_{eff,s} = 88.0$

$r_c = 30.0$

Initial Conditions:

Densities (cm^{-3})

$n_{ihx} = 1 \times 10^{12}$
$n_{ictt} = 1 \times 10^{11}$
$n_{icbt} = 1 \times 10^{11}$
$n_{ic} = 1 \times 10^{12}$
$n_{\alpha} = 1 \times 10^{8}$
$n_{iha} = 5 \times 10^{11}$
$n_{ewa} = 1 \times 10^{11}$
$n_{ehb} = 2 \times 10^{11}$

Temperatures (keV)

$E_{ihx} = 1.0$
$T_{ic} = 0.1$
$T_{ec} = 0.1$
$E_{iha} = 1.0$
$T_{ew} = 1.0$
$E_{ehb} = 1.0$

Other Parameters

$f_{rf} = 0.5$
$T_{eb}/E_{ehb} = 0.8$
$f_s = 0.4$
$\gamma = 2.0$

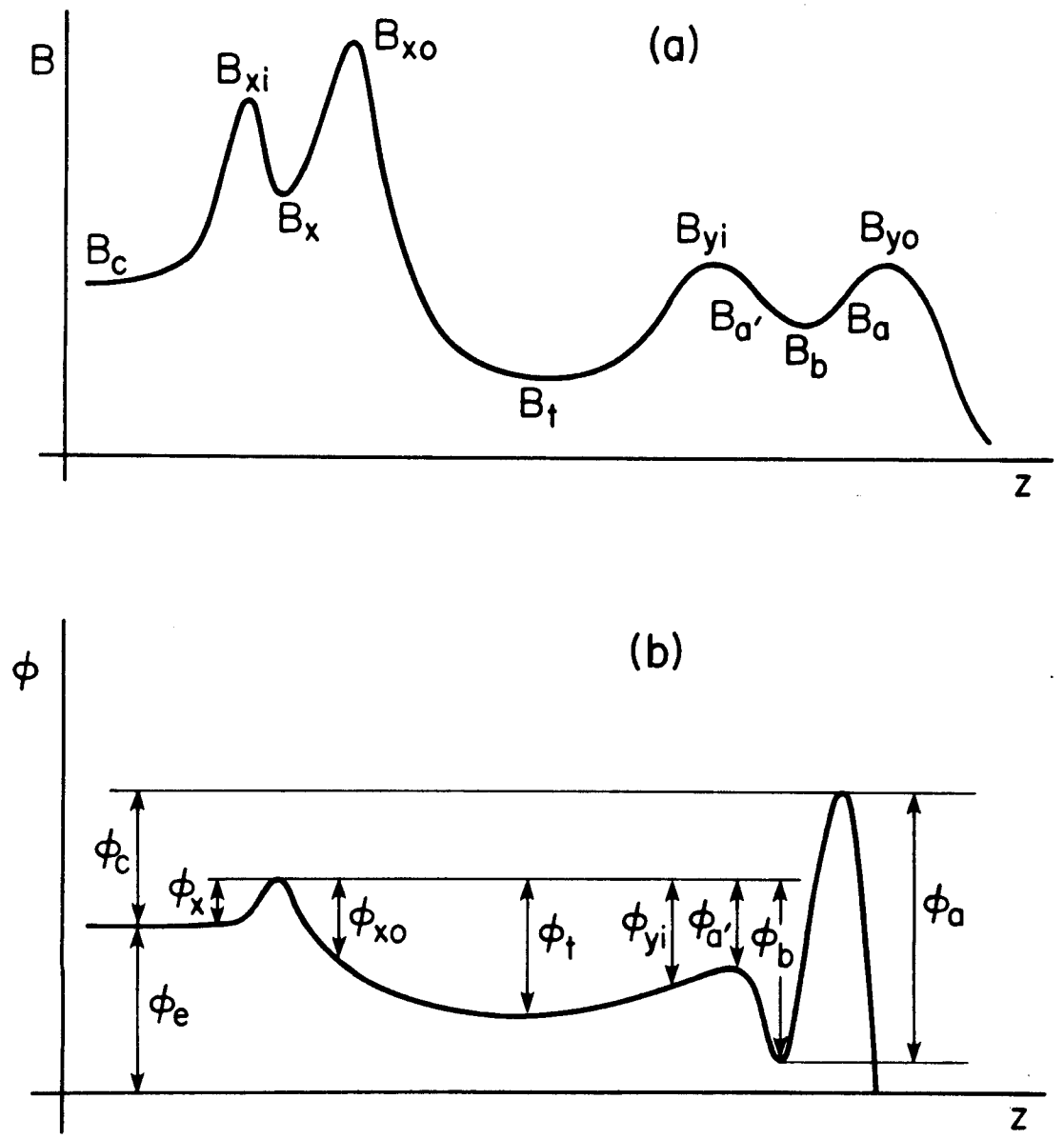

Fig. 1. Axial profiles for the axicell MFTF-B reference case.
(a) Axial magnetic field.
(b) Electrostatic potential.

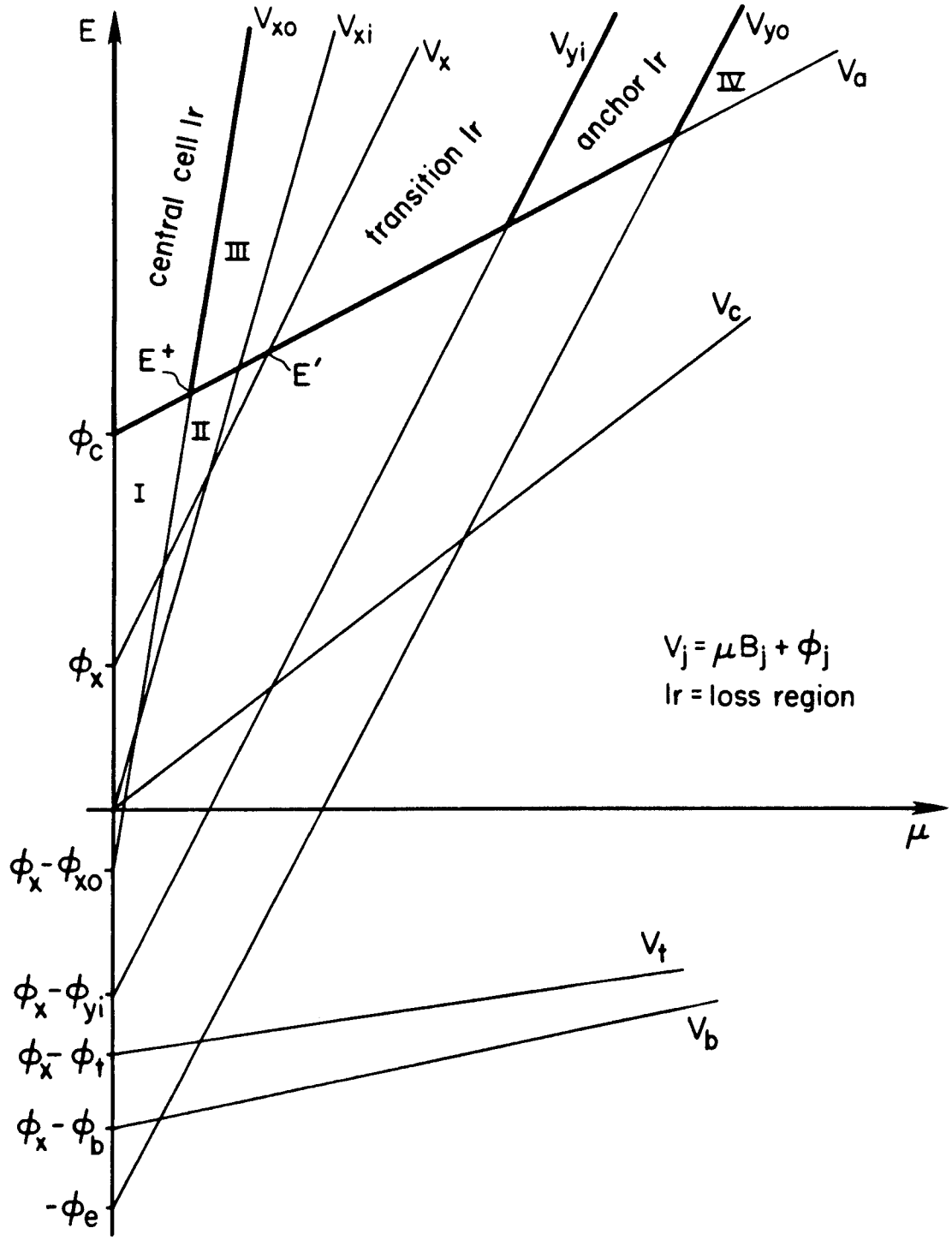

Fig. 2. Ion velocity space (energy vs. magnetic moment) for the axicell MFTF-B reference case.

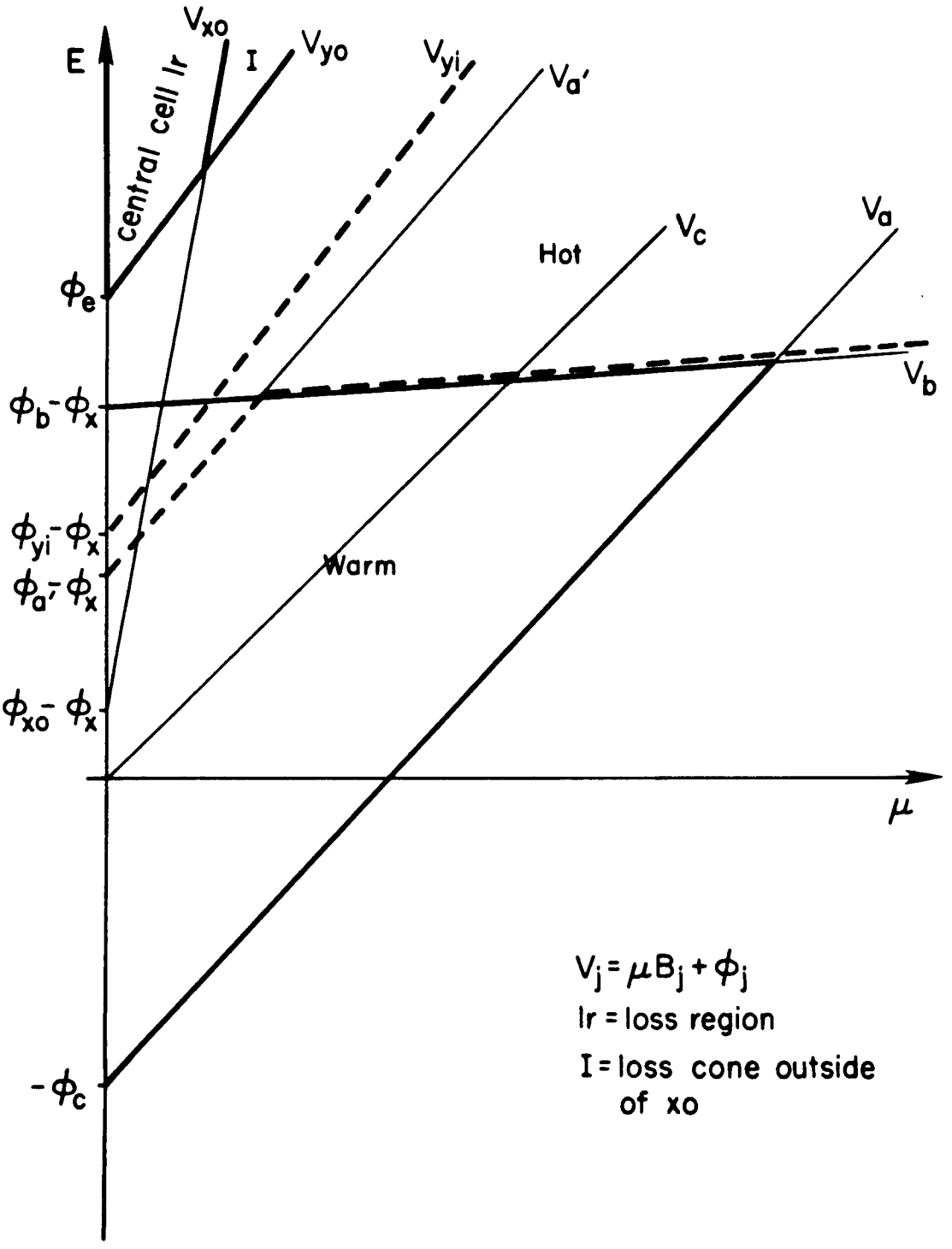

Fig. 3. Electron velocity space (energy vs. magnetic moment) for the axicell MFTF-B reference case.

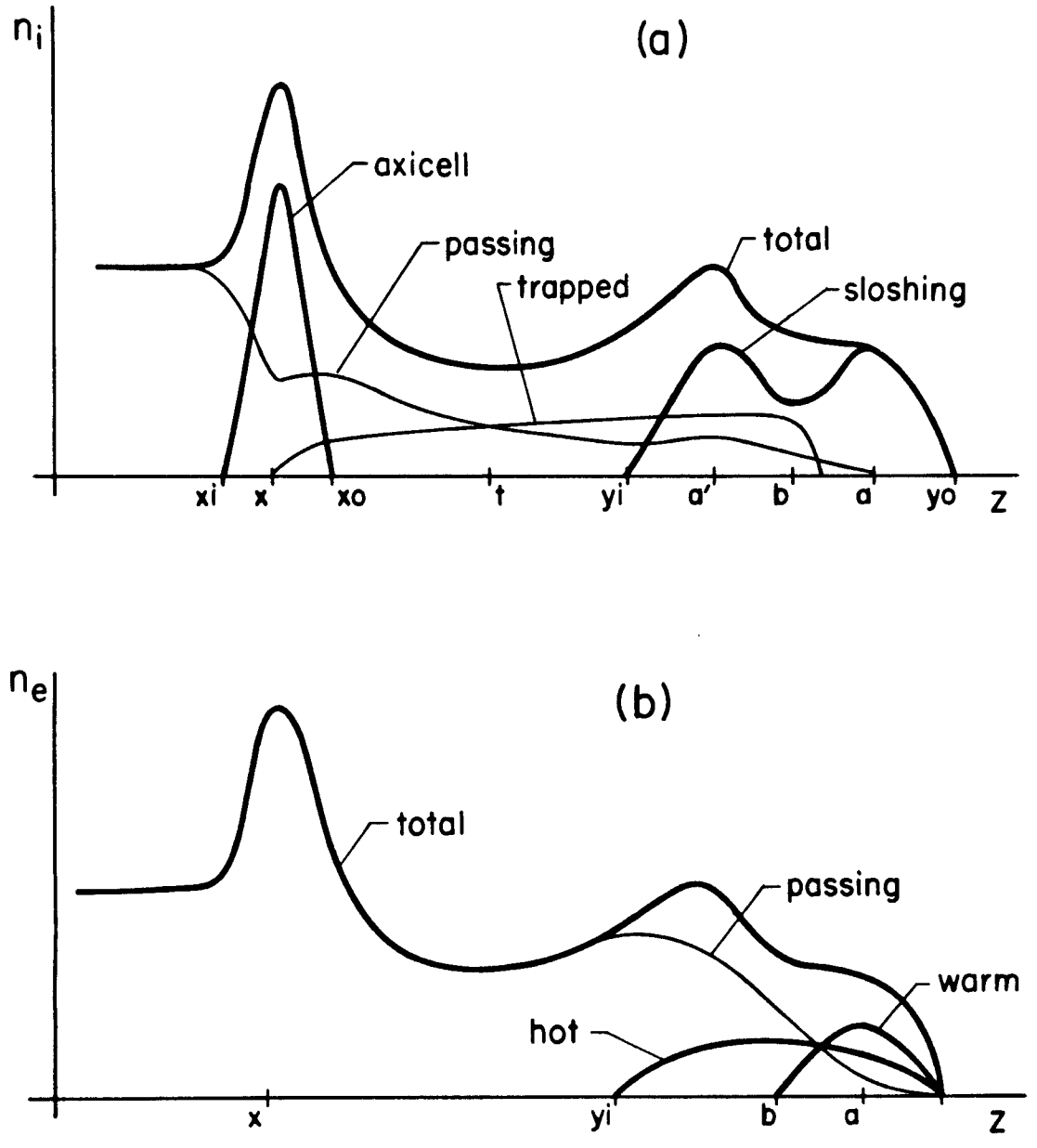

Fig. 4. Axial density profiles for the axicell MFTF-B reference case.
(a) Ions.
(b) Electrons.

Fig. 5. Time evolution of plasma parameters and external sources applied to the plasma during startup.

(a) Temperature or mean energy (keV): 1 - Axicell hot ion mean energy E_{ihx}; 2 - central cell ion temperature T_{ic}; 3 - central cell electron temperature T_{ec}; 4 - sloshing ion mean energy E_{iha}; 5 - plug warm electron temperature T_{ew}; 6 - barrier hot electron mean energy E_{ehb}.

(b) Densities (cm^{-3}): 1 - axicell hot ions n_{ihx}; 2 - transition trapped ions n_{ictt}; 3 - barrier trapped ions n_{icbt}; 4 - central cell ions n_{ic}; 5 - central cell alpha particles n_{α}; 6 - plug sloshing ions n_{iha}; 7 - plug warm electrons n_{ewa}; 8 - barrier hot electrons n_{ehb}.

(c) Total densities (cm^{-3}): 1 - central cell n_c; 2 - axicell n_x; 3 - transition region n_t; 4 - barrier n_b; 5 - plug n_a.

(d) Beta parameters: 1 - central cell; 2 - axicell; 3 - transition; 4 - barrier; 5 - plug.

(e) Ambipolar potentials (keV): 1 - central cell floating potential ϕ_e; 2 - axicell midplane ϕ_x; 3 - axicell magnetic field peak ϕ_{xo}; 4 - transition ϕ_t; 5 - barrier ϕ_b; 6 - plug ϕ_c.

(f) Confinement products (s/cm^{-3}): 1 - central cell ions; 2 - central cell electrons; 3 - plug sloshing ions; 4 - axicell hot ions; 5 - barrier hot electrons; 6 - plug warm electrons.

(g) Pumping parameters: 1 - transition region g_t; 2 - barrier region g_b and ion trapping rates (A); 3 - transition region; 4 - barrier region.

(h) Particle sources (A): 1 - axicell neutral beam injected source; 2 - axicell neutral beam absorbed source; 3 - transition neutral beam injected source; 4 - transition neutral beam absorbed source; 5 - barrier neutral beam injected source; 6 - barrier neutral beam absorbed source.

(i) Particle sources (A): 1 - sloshing ion neutral beam injected source; 2 - sloshing ion neutral beam absorbed source; 3 - central cell neutral beam injected source; 4 - central cell neutral beam absorbed source; 5 - central cell gas injected source; 6 - central cell gas absorbed source.

(j) Neutral beam power (MW) injected into the plasma: 1 - axicell; 2 - transition; 3 - barrier; 4 - sloshing ion; 5 - central cell.

(k) RF power (MW) injected and absorbed in the plasma: 1 - external power applied to central cell ions; 2 - power absorbed by central cell ions; 3 - external power applied to plug electrons; 4 - power absorbed by plug electrons; 5 - external power applied to barrier electrons; 6 - power absorbed by barrier electrons.

(l) 1 - fusion power produced (MW); 2 - total power injected into the plasma (MW); 3 - total power absorbed by the plasma; 4 - multiplication factor q.

FIGURE 5

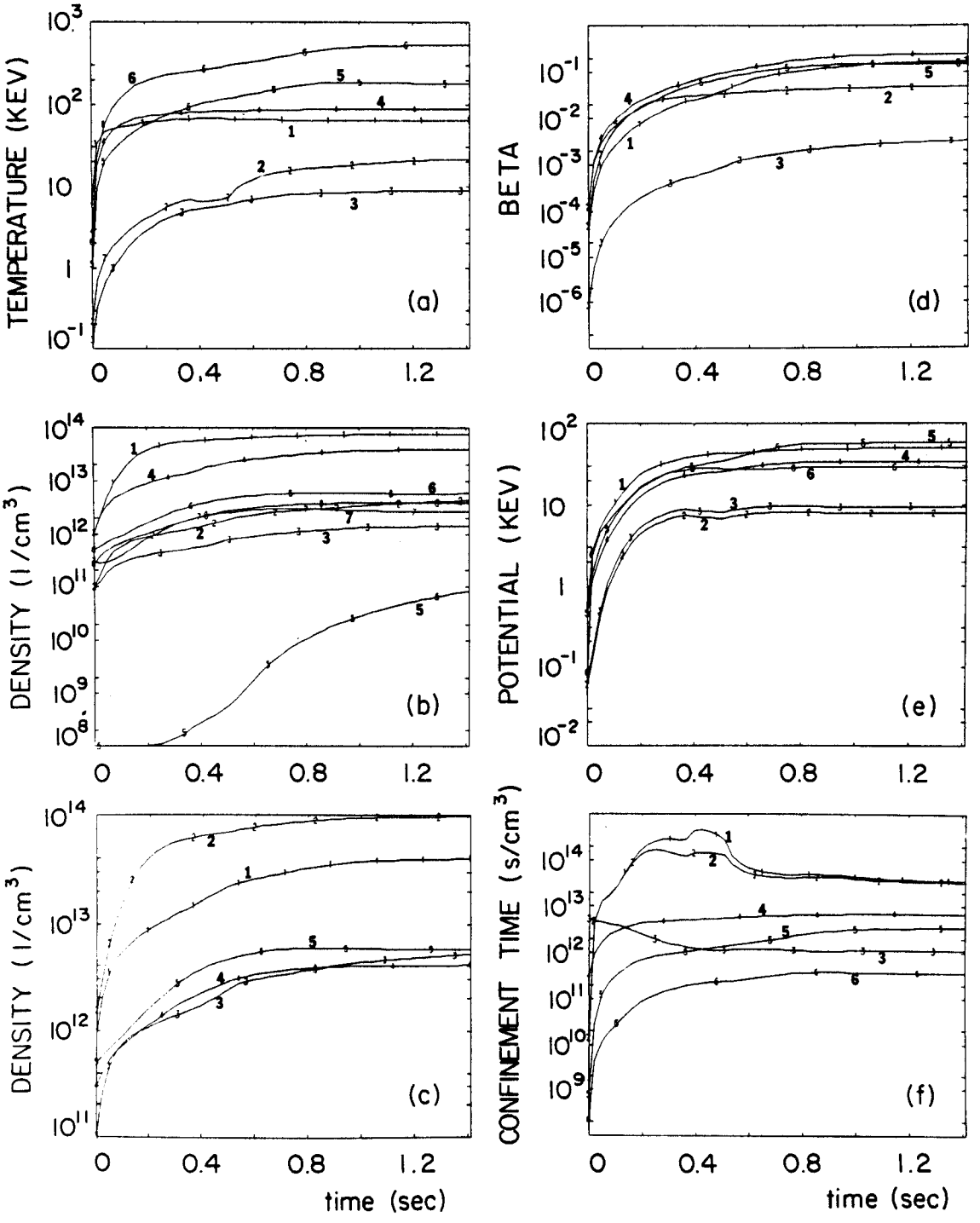
TEMPERATURE (KEV)
(a)
BETA
(d)
DENSITY (1/cm³)
(b)
POTENTIAL (KEV)
(e)
DENSITY (1/cm³)
(c)
CONFINEMENT TIME (s/cm³)
(f)
time (sec)
time (sec)

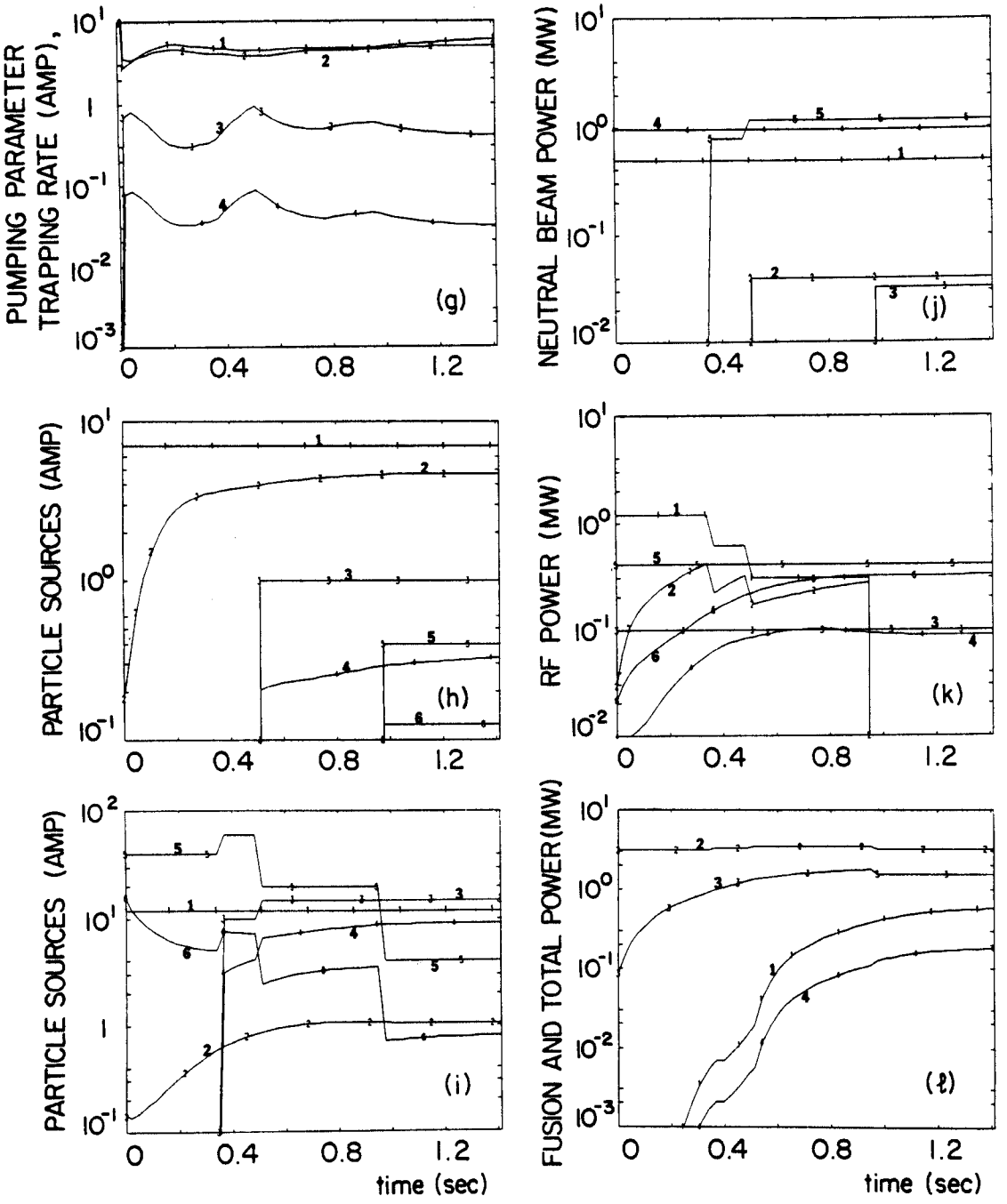
PUMPING PARAMETER TRAPPING RATE (AMP),
(g)
NEUTRAL BEAM POWER (MW)
(j)
PARTICLE SOURCES (AMP)
(h)
RF POWER (MW)
(k)
PARTICLE SOURCES (AMP)
(i)
FUSION AND TOTAL POWER(MW)
(ℓ)
time (sec)
time (sec)